

Submitted to the IRUG Annual Meeting of 2002

Development and Assessment of the Appendix K Version of RELAP5-3D for LOCA Licensing Analysis

Thomas K.S. Liang,
Chin-Jang Chang, Huan-Jen Hung
Nuclear Engineering Division
Institute of Nuclear Energy Research
P.O. Box 3-3, Lung-Tan, Taiwan
Phone: +886-3-4711400 ext 6087
Fax: +886-3-4711404

Abstract

In light water reactors, particularly the pressurized water reactor (PWR), the severity of a LOCA would limit how high the reactor power can operate. Although the best-estimate LOCA licensing methodology can provide the greatest margin on the PCT evaluation during a LOCA, it generally takes much more resources to develop. Instead, implementation of evaluation models required by the Appendix K of 10 CFR 50 upon an advanced thermal-hydraulic platform such as RELAP5, TRAC, et al., also can gain significant margin for the PCT calculation. Through compliance evaluation against the Appendix K of 10 CFR 50, all of the required evaluation models have been implemented into RELAP5-3D. To verify and assess the development of the Appendix K version of RELAP5-3D, nine kinds of separate-effect experiments and eight sets of LOCA integral experiments were adopted. Through the assessments against separate-effect experiments, the success of the code modification in accordance with the Appendix K of 10 CFR 50 was demonstrated. Furthermore, four sets of typical integral LBLOCA experiments from LOFT and Semi-scale have also been applied to evaluate the integral performance of the Appendix K version of RELAP5-3D. The PCTs predicted by the EM models were greater than the one from both BE calculation and experimental measurements in the whole LBLOCA history with the conservatism ranged from 70-260 °K associated with different operating power and scale. It is worth to note that the uncertainty of PCT evaluated by TRAC-PF1 for a generic Westinghouse four loop RESAR-3S plant was quantified to be 158.3°K. The reasonable conservatism of the integral performance of the newly developed Appendix K version of RELAP5-3D was clearly demonstrated and it can analyze all the phases of both LBLOCA and SBLOCA in one code.

1. Introduction

The Loss of Coolant Accident (LOCA) is one of the most important design basis accidents (DBA). In light water reactors, particularly the pressurized water reactor (PWR), the severity of a LOCA would limit how high the reactor power can operate. In the regulatory analysis^[1], it was estimated that if the peak cladding temperature (PCT) during a LOCA decreases by 100°F, it would be possible to raise the plant power by 10%. The revision of 10 CFR50.46 in 1988 stated that two kinds of LOCA licensing approaches can be accepted, namely the **Realistic** and **Appendix K** methodologies. The realistic licensing technique describes the behavior of the reactor system during a LOCA with best estimate (BE) codes. However, the BE analysis method and inputs must be identified and assessed so that the uncertainties in the calculated results can be estimated to a high confidence level. Alternatively, an ECCS evaluation model (EM) also can be developed in conformance with the required and acceptable features of the Appendix K of 10 CFR 50. The Appendix K approach will guarantee the conservatism of the calculation results, instead of answering the analytical uncertainty. It is widely believed that the realistic approach can more precisely calculate the sequences of a LOCA accident, and therefore provides a greater margin for the PCT evaluation. However, the development of the realistic LOCA methodology is long and costly, and the safety authority is highly demanding in their approach to evaluate uncertainties. For instance, Westinghouse took about 50 man-years over 10 years to develop their best-estimate large break LOCA methodology, and it is the only company to date that has acquired the final approval from the U.S. regulatory authority in 1995 using the new realistic large break LOCA methodology.

Regarding the Appendix K LOCA methodology, it is quite interesting that the advanced codes generally calculated a significantly lower PCT than the early ones for the same set of conditions required by Appendix K of 10 CFR 50. For instance, the PCT of Taiwan's Maanshan Nuclear Power Plant calculated by the latest Westinghouse Evaluation Model BASH^[2] is 445°F (2170°F - 1725°F) lower than that of 1981's

calculation^[3].

Although a realistic LOCA methodology can generally provide a greater margin for PCT evaluation, Appendix K requirements along with an advanced thermal-hydraulic platform still can offer significant margin and can be developed with fewer resources. RELAP5/MOD1 has been successfully modified to serve as a LOCA licensing analysis tool in accordance with the Appendix K of 10 CFR 50 by Yankee Atomic Electric (RELAP5/YA^[4]) in the early 80's and similarly, the RELAP5/MOD2 has also been modified by Babcock & Wilcox (RELAP5/MOD2-B&W^[5]) in the late 80's. It is worth to note that previous LOCA packages usually involve several codes to cover the whole phases of both large and small break LOCAs. For instance, regarding the B&W's LOCA package, RELAP5/MOD2-B&W calculates the Blowdown and BEACH^[6] calculates Refill and Reflood with flooding rate calculated by another REFLOD3B code^[7].

To develop a new Appendix K LOCA licensing tool using the most advanced version of RELAP5, namely RELAP5-3D^[8], a program was launched by INER (Institute of Nuclear Energy Research, Taiwan) with sponsorship from Taiwan Power Company. This LOCA program consists of six sequential phases of work^[9] which includes: (1) RELAP5-3D compliance evaluation and EM models as well as assessment data collection; (2) Individual model implementation and stand-alone verification; (3) Model integration to generate the Appendix K version of RELAP5-3D (RELAP5-3D/K); (4) Integral assessment of the new developed RELAP5-3D/K; (5) LOCA licensing analysis with RELAP5-3D/K for the Taiwan's Maanshan Power Plant; and (6) Licensing submittal covering both RELAP5-3D/K development and plant specific application for approval.

In this paper, all of the required evaluation models have been implemented into RELAP5-3D. To verify and assess the development of the Appendix K version of RELAP5-3D, nine kinds of separate-effect experiments were adopted. Through the assessments against separate-effect experiments, the success of the code modification in accordance with the Appendix K of 10 CFR 50 was demonstrated. Furthermore, four sets of typical integral LBLOCA experiments from LOFT and Semi-scale have also been applied to evaluate the integral performance of the Appendix K version of RELAP5-3D.

Besides, sensitivity studies on important parameters including discharge coefficient, onset of reflow, incore vertical stratification, abrupt area change on incore cross flow junction, break nodding and time step also have been performed.

2. Code Modifications and Assessments to Satisfy Requirements of Appendix K of 10 CFR 50

The best-estimate version of RELAP5-3D was modified and assessed to fulfill requirements set forth in the Appendix K of 10 CFR 50. Separate-effects experiments were applied to assess specific code models and assure each modification working properly. The separate-effects assessment cases for each modification are summarized in Table 1.

2.1 Metal-Water Reaction Rate

Since melting of fuel cladding is not the applicable domain, the parabolic rate law from the Baker-Just model^[10] would be applied to calculate the fuel oxidation from zirconium-water reaction:

$$\left(\frac{dr}{dt}\right) = \frac{B}{R_0 - r} \text{Exp}\left(-\frac{G}{T_s}\right) \quad (3.1)$$

The above original form of Baker-Just model was re-derived, and the final form used for coding is:

$$AP = 6.98 \times 10^{-5} \times \text{EXP}\left(\frac{-22898.8}{T_s}\right) \Delta t \quad (3.2)$$

$$DRP1 = (DRP^2 + AP)^{1/2} \quad (3.3)$$

Once the oxidation thickness has been evaluated, the associated amount of reaction heat added to the cladding and hydrogen generation also would be calculated. The Cathcart data^[11] was used to assess the implementation of the Baker-Just models into RELAP5-3D. Cathcart measured the isothermal reaction rates of Zircaloy-4 tubes in steam at elevated temperatures. After the specified oxidation time, the tube was removed and the oxide thickness was measured using standard metallographic techniques. Typical assessment calculation is shown in Figure 1. It can be seen that at a higher bath temperature (1500°C), the conservatism of the Baker-Just model is very clear.

2.2 Discharge Model

The Moody model for the calculation of two phase choked flow and the Henry Hauske model for the single phase liquid choked flow were added to RELAP5-3D to make a break flow evaluation model. Regarding applying the Moody model, the stagnation conditions (p_o , h_o) need to be derived from the cell center immediately upstream of the exit plane. The stagnation enthalpy can be calculated from the cell center properties as:

$$h_0 = \left(h_f + \frac{v_f^2}{2}\right)(1-x) + \left(h_g + \frac{v_g^2}{2}\right)x \quad (3.4)$$

where the local enthalpies, fluid velocities and flow quality are evaluated at the equilibrium condition at the cell center. By assuming an isentropic process, the stagnation pressure can then be obtained from the local entropy defined by the cell center properties and the stagnation enthalpy through steam table iteration:

$$P_o = P_o(h_o, s(h, P)) \quad (3.5)$$

Data from Marviken Test 22^[12] was used to assess the implementation of the Moody model. Marviken Test 22 was a full-scale critical flow test. The break was connected to the bottom of a large pressure vessel. The pressure vessel, which was originally part of the Marviken Nuclear Power Station in Sweden, was 5.2 meters in diameter and 24.6 meters tall. The vessel initially contained regions of subcooled liquid, saturated liquid and a steam dome. The assessment calculations against measured break flow are shown in Figure 2. The conservatism of the Moody model in two-phase choked flow was demonstrated.

2.3 ECC Bypass Model

During the ECC bypass period, the emergency coolant would be held in the upper downcomer region. Those ECC water would accumulate in the inlet lines, and then leave RCS through the break without taking decay heat from the reactor core, until the vapor

flow from the core can no longer sustain the water in the downcomer. The downcomer flooding model derived from the UPTF full-scale test^[13] was applied to determine when the ECC water could penetrate the downcomer through the RELAP5-3D regular CCFL input process. The UPTF downcomer flooding model is:

$$j_g^{*1/2} + 2.193j_f^{*1/2} = 0.6208 \quad (3.6)$$

According to the requirement, before the end of the bypass period all the injected ECC water needs to be removed from the system. To fulfill the ECC subtraction requirement, a set of time dependent junction and volume (TMDPJUN, TMDPVOL) would be connected to the cold leg of the broken loop close to the downcomer. Equal amount of injected ECC water will be forced to be on-line removed from the reactor system by this artificial set of TMDPJUN and TMDPVOL. The boron transport calculation of RELAP5-3D can indicate when the end of ECC bypass takes place. This boron model will trace the transport of the borated ECC water. Once the borated ECC water penetrates the downcomer and reaches the lower plenum, a signal of the end of ECC bypass will be generated and the ECC subtraction scheme via the TMDPJUN and TMDPVOL will be automatically terminated. The comparison of actual injected ECC water in the LOFT L2-5^[14] and the one calculated by the Appendix K model is shown in Figure 3.

2.4 Critical Heat Flux during Blowdown

The set of three Appendix K CHF correlations used in RELAP4/MOD7^[15] would be adopted, which includes B&W-2, Barnett and Hughes (modified Barnett) correlations, to cover the pressure range of interest. For the high-pressure range ($P > 10.34$ MPa), B&W-2 was applied; for the medium pressure range (8.96 MPa $> P > 6.89$ MPa), Barnett correlation was applied; for the low-pressure range ($P < 5$ MPa), the modified Barnett was adopted. For pressures between ranges, interpolation by pressure was applied to calculate the correspond CHF:

$$q_{CHF} = \frac{(P_H - P)q_{CHF_L} + (P - P_L)q_{CHF_H}}{P_H - P_L} \quad (3.7)$$

where index H and L represent the high and low ends of the interpolation range. Rod

bundle heat transfer tests^[16] performed in the Thermal-Hydraulic Test Facility (THTF) at Oak Ridge National Laboratory (ORNL) were used to assess the CHF model and film boiling heat transfer. These tests were performed using an 8 × 8 fuel bundle. The rod geometry was representative of 17 × 17 fuel bundles, and the full-length bundle was electrically heated and had uniform axial and radial profiles. Three tests were used for assessment the CHF calculation, which include tests 3.07.9B, 3.07.9N and 3.07.9W. The range of conditions during this test was representative of those expected during a large break LOCA. A typical comparison of the location first experiencing CHF is shown in Figure 4. It can be seen that the CHF location predicted by the EM models was conservatively lower.

2.5 Post-CHF Heat Transfer during Blowdown

Two correlations suggested by Appendix K of 10 CFR 50 were adopted to calculate film boiling and transition boiling heat transfer. For the stable film boiling, Groeneveld 5.7 was applied, while the McDonough-Milich-King correlation was used for transition boiling heat transfer. Once CHF has occurred, the greater heat flux would be applied which were calculated by the either the film boiling or transition boiling correlations. As stated in Appendix K, the Groeneveld correlation shall not be used in the region near its low-pressure singularity. As suggested by INEEL^[17], for high flow ($j_g^{*1/2} + j_f^{*1/2} > 1.36$ for up flow, $j_g^{*1/2} + j_f^{*1/2} > 3.5$ for downflow) if pressure is less than 1.38 MPa, the modified Dittus-Boelter correlation can be used to replace the Groeneveld correlation. If the core flow is not high, the modified Bromley correlation by Hsu with convection can be used to correct the low-pressure singularity. Typical assessments against THTF tests for film boiling heat transfer of the EM model is shown in Figure 5. As for the assessment of transition boiling heat transfer, THTF transition test with power ramping (THTF-303.6AR) was adopted. A typical comparison is shown in Figure 6.

2.6 Prevention from Returning to Nucleate Boiling and Transition Boiling Heat

Transfer prior to Reflood

As required by Appendix K, during the blowdown phase once CHF occurs, transition boiling and nucleate boiling heat transfer shall not be reapplied for the remainder of the LOCA blowdown, unless the reflood phase of the transition has been entered. Assessment of the artificial prevention algorithm is shown in Figure 7. This figure depicts the mode change with and without the prevention algorithm. It can be seen that nucleate boiling heat transfer was successfully prevented by the algorithm which modifies the existing heat transfer logic.

2.7 Core Flow Distribution during Blowdown

To fulfill the requirement of taking into account cross flow between regions and any flow blockage calculated to occur during blowdown as a result of cladding swelling or rupture, the feature of the cross flow junction of the RELAP5-3D would be applied. In cross flow junctions, the transverse momentum convection terms are neglected. Therefore, there is no transport of x-direction momentum due to the flow in the transverse direction. To assess the calculation of core flow distribution under flow partial blockage, two EPRI flow blockage tests^[18] were adopted in which single-phase liquid and two-phase air/water were used for a range of blockages and flow conditions. The comparisons of the calculated channel pressure distribution for the unblocked channel of the two-phase test against measurements is shown in Figure 8.

2.8 Reflood Rate for PWRs

According to Appendix K of 10 CFR 50, the calculated carryover fraction and mass in bundle needs to be verified against applicable experimental data. In the existing PSI reflood model^[19] of RELAP5-3D, the modified Bestion correlation was used for interfacial drag in vertical bubbly-slug flow at pressures below 10 bars to replace the EPRI correlation. Above 20 bars the EPRI correlation was used. Between 10 and 20 bars the interfacial drag was interpolated. To assess the performance of the PSI model in the best estimate version of the RELAP5-3D, five FLECHT-SEASET tests^[20] (31504, 31203,

31302, 31805 and 33338) were adopted. For the first four forced reflood tests, the flooding rates ranged from 0.81 inch/s to 3.01 inch/s. As for the last gravity-driven reflood test, the flooding rate was up to 11.8 inch/s during the accumulator injection period. Typical assessments were shown in Figures 9 and 10. Through the assessments against five reflood tests, it was found that the PSI model could predict the flooding rate reasonable well but with enough conservatism.

2.9 Refill and Reflood Heat Transfer for PWRs

During reflood phase, the RELAP5-3D PSI model was adopted to fulfill the Appendix K requirement for a flooding rate greater than 1 inch/sec with necessary modifications. In the PSI model, a modified Weisman correlation calculating the heat transfer to liquid and a modified Dittus-Boelter correlation calculating the heat transfer to vapor replace the Chen transition boiling correlation. As for film boiling, heat transfer to liquid uses the maximum of a film coefficient contributed by the modified Bromley correlation, and a Forslund-Rohsenow coefficient. In addition, radiation to droplets is added to the final film-boiling coefficient to liquid. The heat transfer to vapor for film boiling is the same as the one for transition boiling, which was calculated by the modified Dittus-Boelter ($h_{Ditt} \alpha_g$). As required by the Appendix K of 10 CFR 50, when the flooding rate is less than 1 inch/s, only steam cooling in the PSI model was allowed. Assessment calculations were performed to against the five FLECHT SEASET tests discussed above. To bound the peak cladding temperature (PCT) span on each measured fuel rods at the same elevation, the calculated heat transfer coefficient calculated by the original PSI model was reduced by a factor of 0.6 for the flooding rate greater than 1 inch/sec to ensure reasonable conservatism. Typical comparison of the PCTs is shown in Figures 11. While the comparison of heat transfer coefficients is shown in Figures 12.

3. Assessment against Integral LBLOCA Experiments

Totally 8 sets of integral LOCA experimental data would be applied to verify the overall conservatism of the newly developed Appendix K version of RELAP5-3D. Experimental conditions of 8 tests were summarized in Table 2. In this paper only assessment results against integral LBLOCA experiments have been addressed to demonstrate the integral performance of RELAP5-3DK/INER on LBLOCA analysis. The detailed assessment results against L2-5^[21] are discussed in this paper, and figure of merit of other cases are also presented. Besides, sensitivity studies on important parameters including discharge coefficient, onset of reflood, incore vertical stratification, abrupt area change on incore cross flow junction, break nodding and time step also have been performed.

Right after the break in the test of L2-5, break flows from both ends calculated by the EM model were generally larger than the one from BE calculation of RELAP5-3D^[22], as shown in Figure 13. As a result, the system was depressurized faster in EM calculation than the other two, as shown in Figure 14. As required by the Appendix K of 10 CFR 50, effective ECC water calculated by the EM model would be less than the actual amount of water injected to satisfy the ECC bypass requirement. The comparison of the effective ECC water injected into the system from both EM and BE models is shown in Figure 15. It is clear that the amount of ECC water injected into the system calculated by the EM models of RELAP5-3D is delayed and relatively less. As a result, water level in the downcomer calculated by the EM model would descend lower and recover in a later time, as shown in Figure 16.

Removing ECC water during bypass period resulted in a late core reflood in the EM model calculation, as shown in Figure 17. It can be seen that the core inlet liquid void fraction clearly increased at about 40 seconds after the break in the EM calculation, which was about 20 seconds late compared to the BE calculation. Consequently, recovery of reactor average channel coolant mass was predicted to be late too by the EM calculation, as shown in Figure 18. As expected, quench front movements of both hot and average fuel rods predicted by the EM models also depicted a late response

compared to the BE calculation, as shown in Figure 19.

As for the core heat transfer, different heat transfer packages in the EM models are applied for the following three sequential phases of a LBLOCA:

- (1) **Blowdown:** Correlations suggested by the Appendix K as stated in previous section are applied for the core heat transfer, which include the predictions of CHF and post CHF heat transfer. Correlations of B&W2, Barnett and Hughes are applied to calculate CHF for a right range of pressure. Regarding the post CHF heat transfer, Groeneveld 5.7 is applied for the stable film boiling and McDonough-Milich-King correlation is for the transition boiling heat transfer;
- (2) **Refill:** Since ECC water still remains below the core in this phase, steam cooling only is assumed as required by the Appendix K of 10 CFR 50, and Dittus correlation is applied to calculate the steam convection;
- (3) **Reflood:** PSI reflood model will be applied when the flooding rate is greater than 1.0 inch/sec with a reduction factor of 0.6. While steam cooling only is also applied for flooding rate less than 1.0 inch/sec as required by the Appendix K.

The core heat transfer package for the Appendix K version of RELAP5-3D is summarized in Table 3.

The CHF predicted by the EM models is generally smaller than the one from BE models of RELAP5-3D, as shown in Figures 20. As a result, early post CHF heat transfer during blowdown would be resulted in the calculation of EM models. The comparison of heat transfer coefficient on the hot spot is shown in Figure 21. It can be seen that during blowdown, the early reduction of the heat transfer coefficient indicates that the early post CHF was experienced on the hot spot in the EM calculation. While, it also indicates that post-CHF heat transfers from both models are quite compatible during blowdown. As for the heat transfer during refill, owing to the steam cooling assumed in the EM models, the heat transfer coefficient predicted by the EM models is relatively smaller as compared to the one from BE calculation. Regarding the reflood calculation, owing to the reduction factor calibrated by FLECHT SEASET reflood tests, the heat transfer coefficients predicted by the EM model was smaller prior to the quench front. Resulted from the

integral conservatism, particularly the ECC bypass, a late quench was also observed in the EM calculation, as shown in Figure 21.

Considering the peak cladding temperature (PCT), the most important safety parameter required by the 10 CFR 50, the comparison of PCTs between calculations from both EM and BE models as well as the measurement spans within the fuel conduction node are shown in Figure 22. It can be seen that the PCT predicted by the EM models is greater than the values from both BE calculation and measurements in the whole LOCA history. The difference of PCTs between BE and EM calculations is about 150°K. The comparison of PCTs along the hottest rod from both EM and BE calculations is also shown in Figure 23. It indicates the general conservatism of the EM models in each location along the hottest rod as compared to the RELAP5-3D BE models.

To demonstrate the general conservatism of the Appendix k version of RELAP5-3D, the PCT versus time and fuel elevations respectively of assessments against L2-3, LP-LB-1 and S-06-3 are also presented in Figures 24 to 29. It can be seen that RELAP5-3D/K calculates higher PCTs than what from both experiments and BE calculations. The PCTs of all the LBLOCA assessments are plotted against the maximum linear heat generation rate of each cases, as shown in Figure 30, to illustrate the general conservatism of RELAP5-3D/K over different powers and different scales. It can be seen that the resulted PCTs from experiments and BE calculations lie together, while the PCTs from EM calculations are presented with reasonable conservatism. It should be noted that owing to different status of RCP, the results from L2-3 are not included in Figure 30. The PCTs of each case are also summarized in Table 4. The conservatism of PCTs by EM calculations over the experimental measurements ranges from 65.9°K to 259.3°K for different operating power and scale. It is worth to note that because the early rewet by RCP running which was not allowed in the case of L2-3 EM calculation, a relatively higher PCT by the EM calculation was resulted. Regarding the case of S-06-3, because the CCFL model adopted by RELAP5-3D/K was derived from UPTF full-scaled experiments, a prolonged ECC bypass period by 30 seconds was resulted as compared to the BE calculation in the small-scaled S-06-3 experiment. As a result, a relatively higher

PCT was also observed in the S-06-3 assessment. If the UPTF CCFL correlation is replaced by Wallis's, the PCT can be reduced by 50.0 °K, as shown in Figure 31.

Sensitivity studies on important parameter settings are also performed for all the LBLOCA assessments, which include discharge coefficient, liquid void fraction on the core inlet junction to activate reflood calculation, incore volume vertical stratification, abrupt area change on the incore cross flow junction, break nodding size and time step. The results are summarized in Table 5. It was observed that the PCT is not sensitive to those setting except the discharge coefficient. The limiting discharge coefficients vary from 0.75 to 1.0 for different cases.

4. Conclusions

Although the best-estimate LOCA methodology can provide the greatest margin for the PCT evaluation during a LOCA, it generally takes more resources to develop. Instead, implementation of evaluation models required by Appendix K of 10 CFR 50 upon an advanced thermal-hydraulic platform can also gain significant margin on the PCT calculation but with fewer resources. Ten major areas of the current RELAP5-3D have been modified and/or assessed to satisfy requirements set forth in the Appendix K of 10 CFR 50, which included (1) fission product decay, (2) metal-water reaction rate, (3) discharge model, (4) ECC bypass during blowdown, (5) critical heat flux, (6) prevention to return to nucleate boiling and transition during blowdown, (7) post-CHF heat transfer during blowdown, (8) core flow distribution during blowdown, (9) reflood rate calculation for PWRs, and (10) refill and reflood heat transfer for PWRs. Through the separate effect assessments, modifications of each individual area were verified and successes were well demonstrated. The final package of the Appendix K version RELAP5-3D is summarized in Table 6.

Through the assessments against integral LBLOCA experiments, the reasonable conservatism of RELAP5-3D/K calculation was clearly demonstrated in whole area of a LBLOCA event, which covering hydraulics and heat transfer in the phases of **Blowdown**, **Refill** and **Reflood**. Regarding the figure of merit for a LBLOCA analysis, the PCTs calculated by the EM models are about 65.9-259.3 °K greater than the one from experimental measurements associated with different power and scale. However, if the CCFL correlation derived from UPTF experiments were changed to the default Wallis CCFL in the EM models for the S-06-3 calculation, the resulted difference between PCT by EM calculation and PCT from measurements could be reduced from 259.3 to 210.0 °K. It is also worth to note that the uncertainty of PCT of a LBLOCA evaluated by TRAC-PF1 for a generic Westinghouse four loop RESAR-3S plant was quantified to be 158.3°K^[23]. It can be concluded that the newly developed Appendix K version of RELAP5-3D has been successfully conducted with the ability to analyze all the phases of both LBLOCA and SBLOCA in one code, and the reasonable conservatism of the

integral performance of RELAP5-3D/K for LBLOCA was clearly demonstrated.

Nomenclature

r, R_o = radius and original radius of unreacted metal

t = time

$$B = \frac{10^{-6} * A}{2 * \rho_m^2}$$

A = pre-exponential factor, $29.5 * 10^6 (\text{mg}/\text{cm}^2)^2/\text{sec}$

ρ_m = metal density

$$G = \frac{\Delta E}{R}$$

ΔE = activation energy, 45.5 kcal/mole

R = gas constant, 1.987 cal/(mole)(°K)

T_s = oxide surface temperature

DRP1 = the depth the reaction has penetrated the cladding at the end of a time step

DRP = the depth the reaction has penetrated the cladding at the start of a time step

h_o = stagnation enthalpy

h_f = liquid enthalpy

h_g = vapor enthalpy

v_f = liquid velocity

v_g = vapor velocity

x = flow quality

p_o = stagnation pressure

s = entropy

j_g^* = dimensionless gas superficial velocity

j_f^* = dimensionless liquid superficial velocity

q_{CHF} = critical heat flux

p = pressure

Reference

1. U.S. NRC, "Compendium of ECCS Research for Realistic LOCA Analysis," NUREG-1230, April 1987.
2. Westinghouse, "The 1981 Version of the Westinghouse ECCS Evaluation Model Using the BASH Code," WCAP-10266-P-A Revision 2, March 1987.
3. Taiwan Power Company, "Final Safety Analysis Report of Maanshan Nuclear Power Station Units 1 & 2," April 1982.
4. R. Thomas Fernandez, et al., "RELAP5/YA: A Computer Program for Light Water Reactor System Thermal-Hydraulic Analysis," YAEC-1300p, Yankee Atomic Electric Company, October 1982.
5. J.A. Klingerfus, et al., "RELAP5/MOD2-B&W: An Advanced Computer Program for Light Water Reactor LOCA and Non-LOCA Transient Analysis," BAW-10164p, Rev. 1, Bancroft & Wilcox Nuclear Power Group, October 1988.
6. N.H. Shah, et al., "BEACH: Best Estimate Analysis Core Heat Transfer, A Computer Program for Reflood Heat Transfer During LOCA," BAW-10166p, Rev. 2, Bancroft & Wilcox Nuclear Power Group, September 1989.
7. C.K. Nithianandan, et al., "REFLOD3B, Model for Multinode Core reflooding Analysis," BAW-10171p, Rev. 3, Bancroft & Wilcox Nuclear Power Group, September 1989.
8. RELAP5-3D Code Development Team, "RELAP5-3D Code Manual, INEEL-EXT-98-00834," September 1998.
9. Thomas K.S. Liang and Richard R. Schultz, "Development Program of LOCA Licensing Calculation Capability with RELAP5-3D in Accordance with 10 CFR 50," Nuclear Technology, 133, 355-358, March 2001.
10. Louis Baker, Jr. and Louis C. Just, "Studies of Metal-water Reactions at High Temperatures," ANL-6548, May 1962.
11. J.V. Cathcart, et al., "Zirconium Metal-Water Oxidation Kinetics IV. Reaction Rate Studies," ORNL/NUREG-17, August 1977.
12. L. Erickson et al., "The Marviken Full-Scale Critical Flow Tests Interim Report:

Results from Test 22, ” MXC-222, March 1977.

13. Siemens, “Test No. 6 Downcomer Countercurrent Flow Test, Experimental Data Report,” U9 316/88/18, December 1988.
14. C.B. Davis, “Assessment of the RELAP5 Multi-Dimensional Component Model Using Data from LOFT Test L2-5,” INEEL-EXT-97-01325, January 1998.
15. Stephen R. Behling, et al., “RELAP4/MOD7-A Best Estimate Computer Program to calculate Thermal and Hydraulic Phenomena in a Nuclear Reactor or Related System,” NUREG/CR-1998, August 1981.
16. G.L.Yoder, et al., “Dispersed Flow Film Boiling in Rod Bundle Geometry-Steady State Heat Transfer Data and Correlation Comparisons,” NUREG/CR-2435, ORNL-5822, March 1982.
17. Richard R. Schultz and Cliff B. Davis, “Recommended Models & Correlations and Code Assessment Matrix for Creating A 10 CFR 50.46 Licensing-Version of RELAP5-3D,” INEEL/EXT-98-01257, Feb. 1999.
18. A. Tapucu, et al., “Experimental Study of the Diversion Cross-Flow Caused by Subchannel Blockages,” EPRI NP-3459, April 1984.
19. G. Th. Analytis, “Developmental Assessment of RELAP5/MOD3.1 with Separate Effect and Integral Test Experiments: Model Changes and Options,” Nuclear Engineering and Design, 163(1996), 125-148.
20. M. Loftus, et al., “PWR FLECHT SEASET Unblocked Bundle, Forced and Gravity Reflood Task Data Report, NUREG/CR-1531, EPRI NP-1459, June 1980.
21. P.D. Bayless and J.M. Divine, “Experiment Data Report for LOFT Large Break Loss-of-Coolant Experiment L2-5, ” NUREG/CR-2826, EGG-2210, 1982.
22. C.B. Davis, “Assessment of the RELAP5 Multi-Dimensional Component Model Using Data From LOFT Test L2-5, ” INEEL-EXT-97-01325, January 1998.
23. K.R. Katsma, et al., “Quantifying Reactor Safety Margins - Application of Code Scaling, Applicability, and Uncertainty Evaluation Methodology to A LBLOCA,” NUREG/CR-5249, Dec. 1989.

Table 1 Cases for Separate-Effect Assessments

Case	Phenomenon/Model	Applicable Appendix K Section
Cathcart oxidation data	metal-water reaction	I.A.5
Marviken Test 22	critical flow	I.C.1.ab
ORNL THTF Tests 3.07.9B 3.07.9N, 3.07.9W	critical heat flux	I.C.4
ORNL THTF Tests 3.07.9B 3.07.9N, 3.07.9W	film boiling	I.C.5
ORNL THTF Test 3.03.6AR	transition boiling	I.C.5
EPRI flow blockage Run 4 and Run 8	core blockage and cross flow	I.C.7.a
FLECHT-SEASET Tests 31504, 31203, 31302, 31805 and 33338	refill and reflood rates	I.D.3
FLECHT-SEASET Tests 31504, 31203, 31302, 31805 and 33338	refilled and reflood heat transfer	I.D.5

Table 2 Cases for Integral-Effect Assessments

Case	L2-3	L2-5	Lp-Lb-1	S-06-3	L3-7	S-LH-1	IIST	L8-2
Break Size	200%	200%	200%	200%	0.1%	5%	0	23%
Break Location	Cold leg	Cold leg	Cold leg	Cold leg	Cold leg	Cold leg	None	Cold leg
Notes	RCP Running	RCP Tripped	High Power Density	NRC problem	Without Core Heatup	With Core Heatup	Natural Circulation	Restart of RCPs

Table 3 Core Heat Transfer Package of RELAP5-3DK/INER

Phases of LBLOCA	Pre CHF	CHF	Transition Boiling	Film Boiling
Blowdown	Original BE pre-DNB Package of RELAP5-3D	(1) $p > 10.34$ Mpa B&W-2 (2) $6.89 < P$ (Mpa) < 8.96 Barnet (3) $p < 5.0$ Mpa Modified Barnet (4) P between Rages Interpolation by P	McDonough-Milich-King	(1) $p > 13.8$ Mpa Groeneveld 5.7 (2) $p < 13.8$ Mpa - high flow modified Dittus - low flow modified Bromley by Hus
Refill	Only steam cooling allowed	Only steam cooling allowed	Steam convection by Dittus	Steam convection by Dittus
Reflood	Original PSI reflood model	(1) $G < 100$ kg/m ² s Modified Zuber (2) $G > 200$ kg/m ² s Groeneveld (3) $100 < G$ (kg/m ² s) < 200 interpolation by G	Original PSI reflood model	(1) flooding rate > 1 inch/s modified PSI model (2) flooding rate < 1 inch/s steam cooling by Dittus

Table 4 Comparison of PCTs of Each Assessment Case

Cases	Measured PCTs (°K)	PCTs by BE Calculations (°K)	PCTs by EM Calculations (°K)	ΔPCT (PCT_{EM}-PCT_{exp}) (°K)
L2-5	1057.2	998.6	1123.1	65.9
L2-3	898.3	938.1	1094.6	196.3
LP-LB-1	1252.4	1290.5	1343.4	91.0
S-06-3	1061.2	1123.7	1320.5(1271.2*)	259.3 (210.0*)

*: with Wallis CCFL correlation

Table 5 Conservative Settings by Sensitivity Studies

Cases	discharge coefficient	liquid void fraction On core inlet junction	incore vertical stratification	abrupt area change on incore x-flow junction	Break nodding (L/D)	time step (sec)
L2-5	0.75	0. 4 (not sensitive)	ture (not sensitive)	ture (not sensitive)	4.5 (not sensitive)	0. 01 (not sensitive)
L2-3	1.00	0.4 (not sensitive)	true (not sensitive)	ture (not sensitive)	4.5 (not sensitive)	0. 01 (not sensitive)
LP-LB-1	0.90	0. 3 (not sensitive)	true (not sensitive)	ture (not sensitive)	4.5 (not sensitive)	0. 01 (not sensitive)
S-06-3	0.70	0. 4 (not sensitive)	ture (not sensitive)	false (not sensitive)	6.8 (not sensitive)	0. 005 (not sensitive)

Table 6 Final Package of RELAP5-3D to Satisfy the Appendix K of 10 CFR 50

Model Requirement	RELAP5-3D Subroutines	Status
Fission Heat	rrkin & rkin	Apply the existing model of the code
Decay of Actinides	rkin	Apply the existing model of the code
Fission Product Decay	rrkin & rkin	<i>Change to 1971 ANS Standard Model</i>
Metal-Water Reaction Rate	Qmwr	<i>Change to Baker-Just correlation</i>
Swell & Rupture of the Cladding and Fuel Rod Thermal Parameters	madata, gapcon, cplexp, ruplas, plstrn, kloss	Apply the existing model of the code
Discharge Model	Jchoke	<i>Change to Moody model</i>
End of Blowdown	None	<i>Apply the CCFL model suggested by UPTF test along with on-line ECC water subtraction scheme</i>
Frictional Pressure Drops	Fwdrag	Apply the existing model of the code
Momentum Equation Requirements	vexplt (semi-implicit)	Apply the existing model of the code
Critical Heat Flux	chfcal & chftab	<i>Change to B&W-2, Barnett, & modified Barnett correlations</i>
Prevent Return to Nucleate Boiling	Htrcl	<i>Modify the existing heat transfer selection logic</i>
Post-CHF Heat Transfer Correlations: Film Boiling	pstdnb & suboil	<i>Change to Groeneveld 5.7, modified Dittus-Boelter, & modified Bromley correlations</i>
Post-CHF Heat Transfer Correlations: Transition Boiling	Pstdnb	<i>Change to McDonough, Milich, & King correlations</i>
Prevent Return to Transition Boiling Heat Transfer Prior to Reflood	Pstdnb	<i>Modify the existing heat transfer selection logic</i>
Pump Model	Pump	Apply the existing model of the code
Core Flow Distribution During Blowdown		<i>Apply the existing cross-flow junction model of the code by assessments and apply core flow smoothing if necessary</i>
Calculation of Reflood Rate for PWRs	rhtcmp, htrcl, qfmove	<i>Applying the existing PSI model by performing separate-effect assessments</i>
Steam Interactions with ECC Water	eccmxj & eccmxv	Apply the existing model of the code
Refill and Reflood Heat Transfer for PWRs	rhtcmp, htrcl, qfmove	<i>Modify the existing PSI model</i>

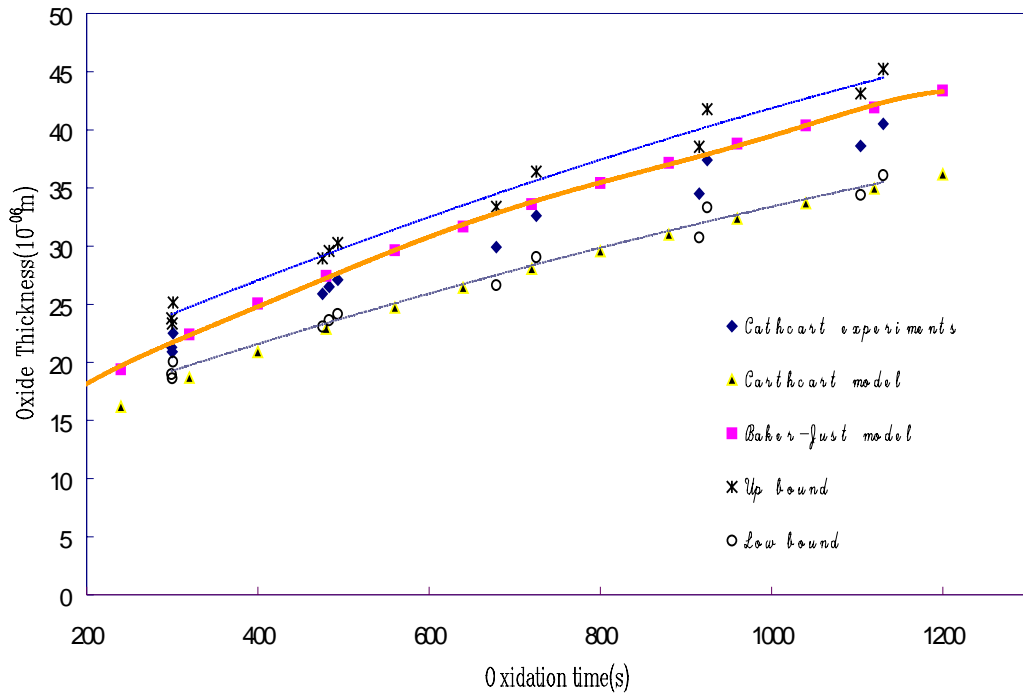


Figure 1. Oxidation Thickness of Zirconium 4 (temperature 1001 °C)

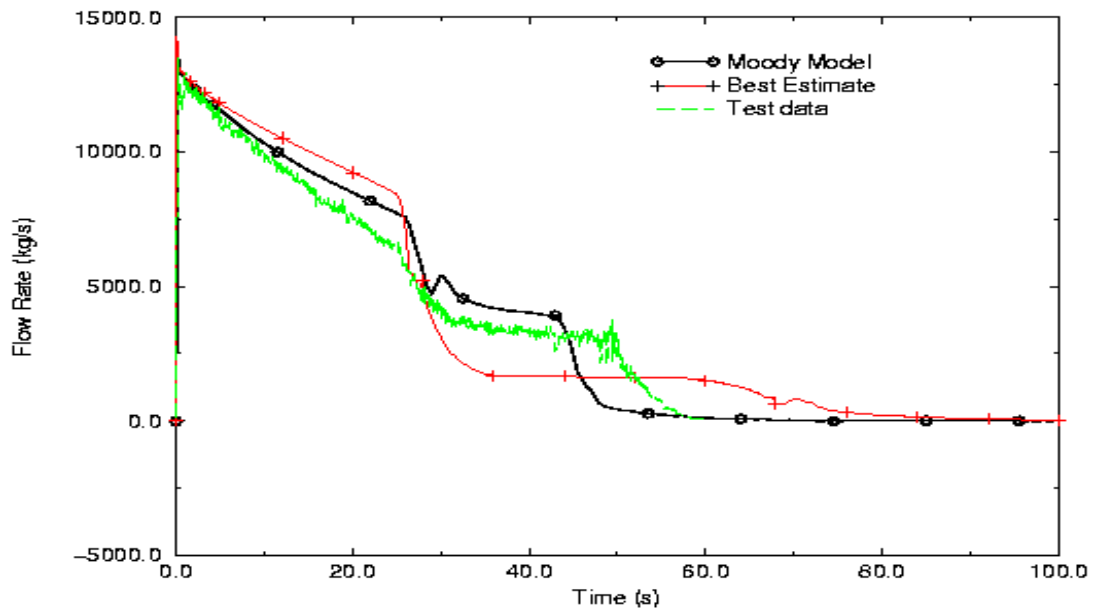


Figure 2. Comparison of Measured and Calculated Break Flow

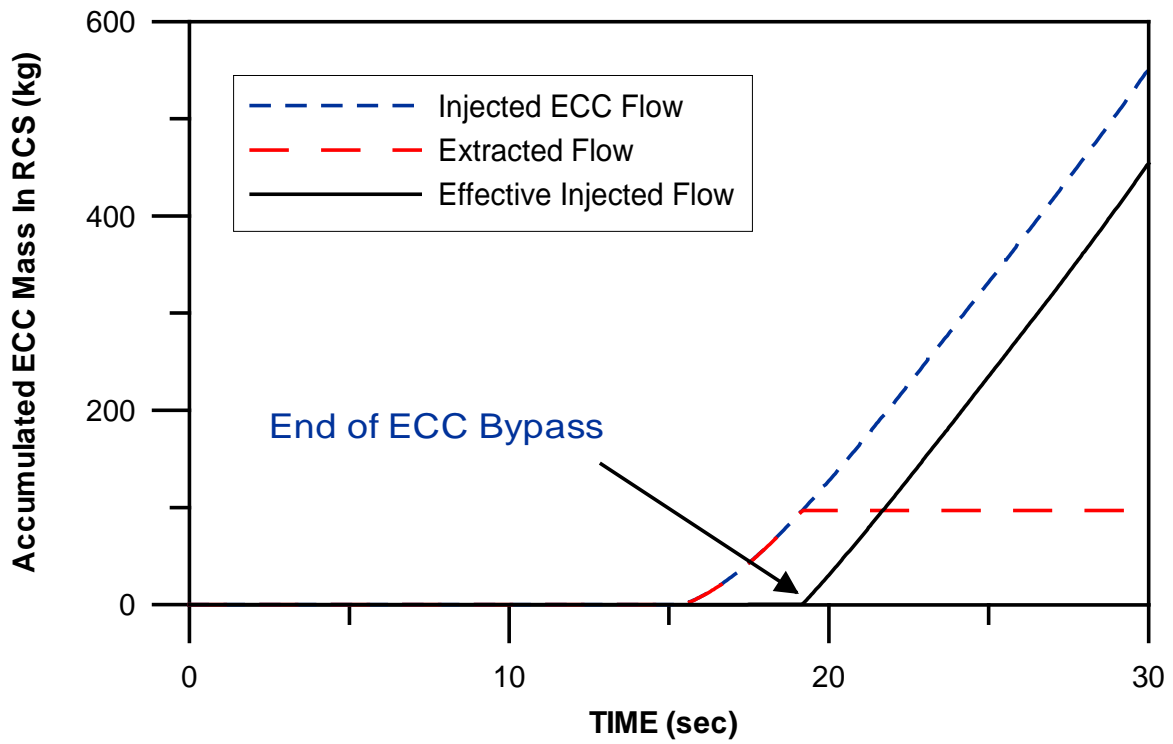


Figure 3. Comparison of Measured and Calculated ECC Water

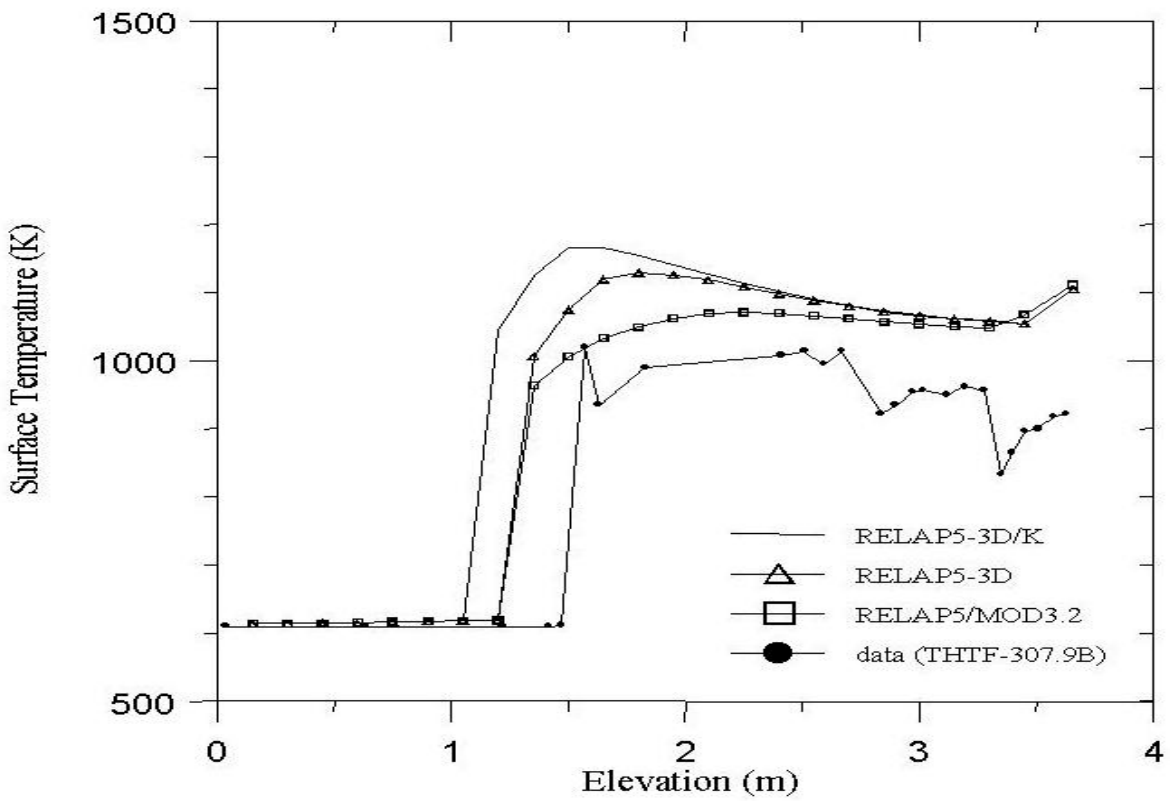


Figure 4. Comparison of Measured and Calculated Temperature Distributions for CHF Assessment

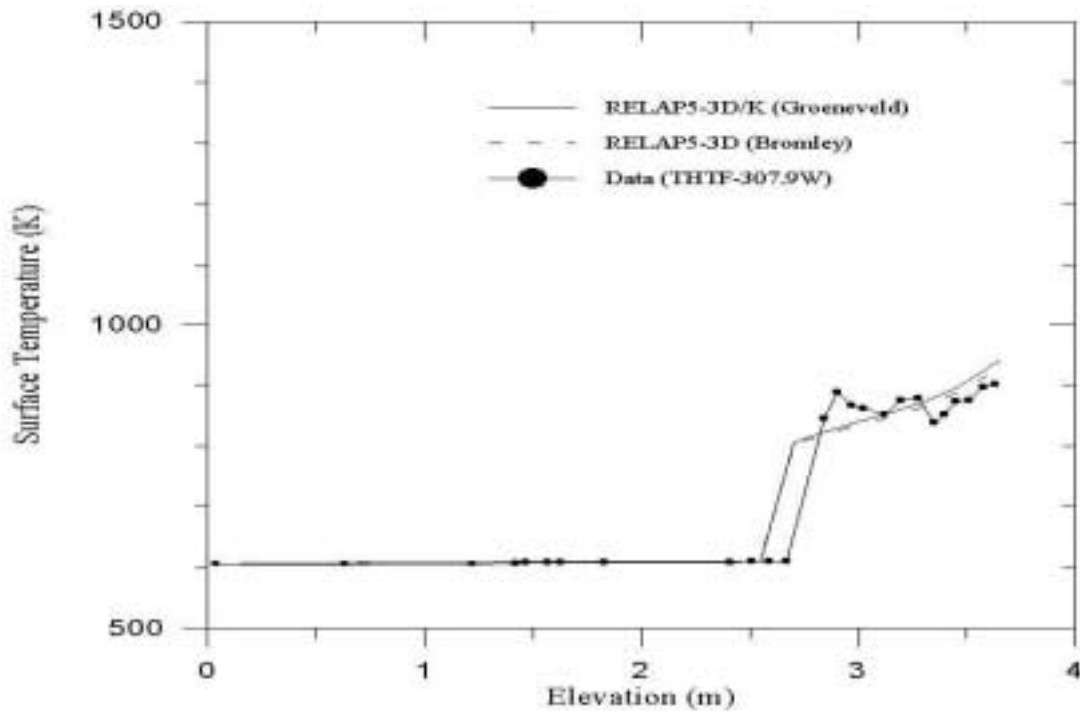


Figure 5. Comparison of Measured and Calculated Temperature Distributions for Film Boiling Assessment

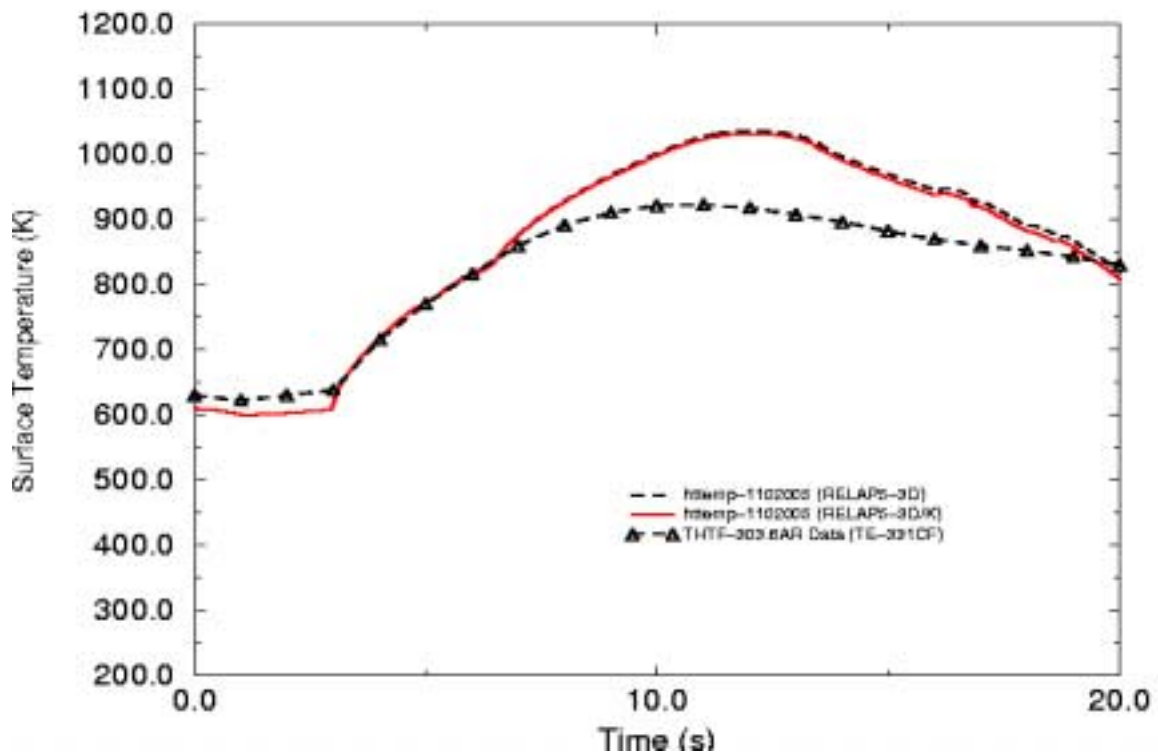


Figure 6. Comparison of Measured and Calculated Temperature Changes for Transition Boiling Assessment

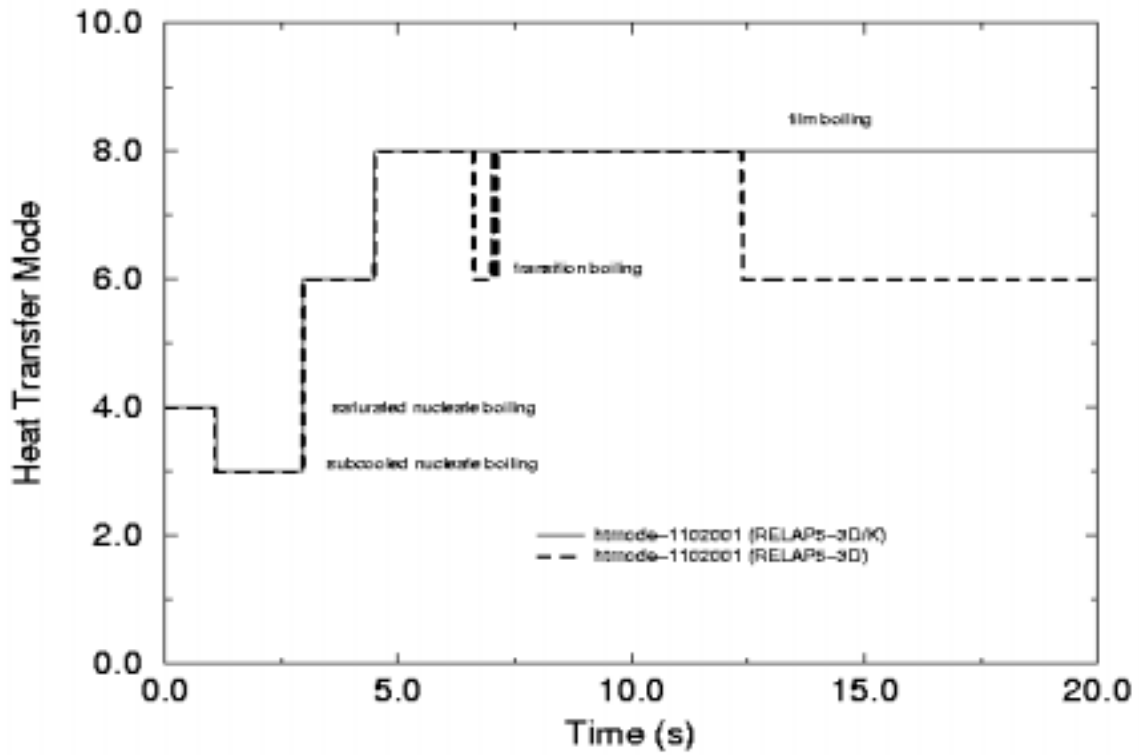


Figure 7. Heat Transfer Mode Calculated by the Modified RELAP5-3D

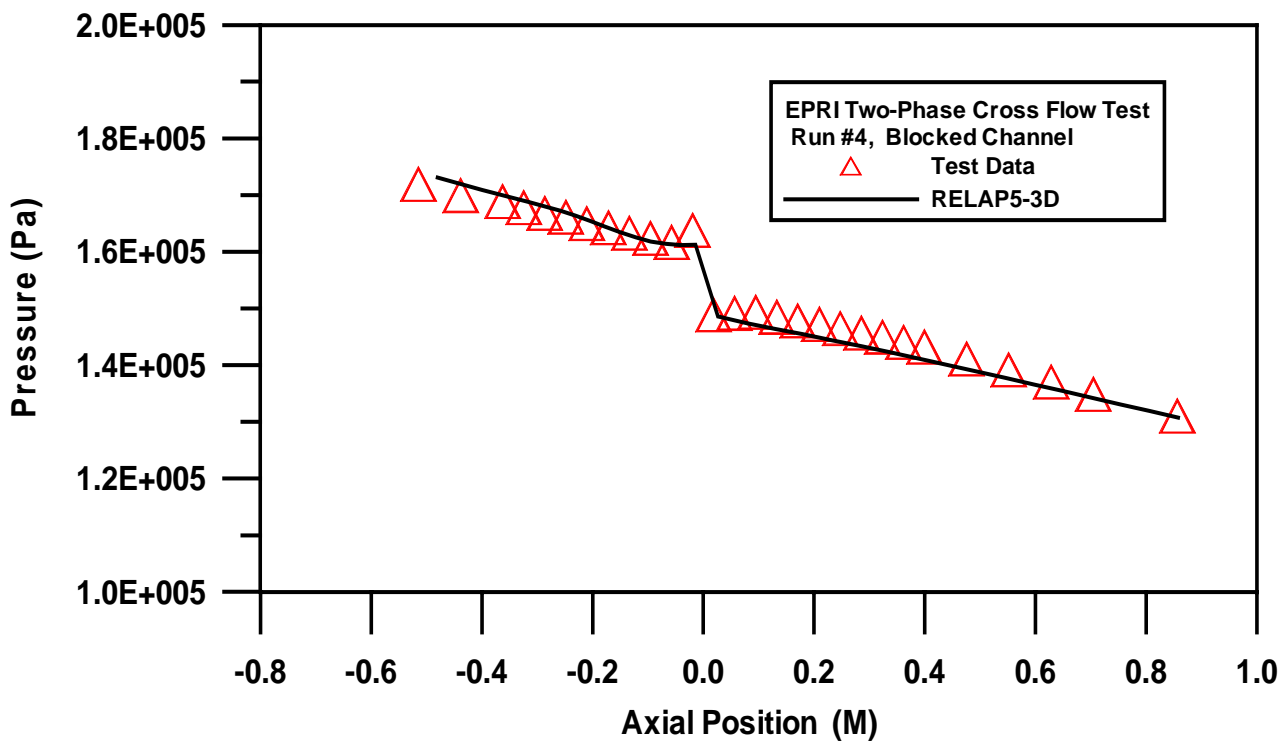


Figure 8. Comparison of Measured and Calculated Pressure Distributions of the Blocked Channel

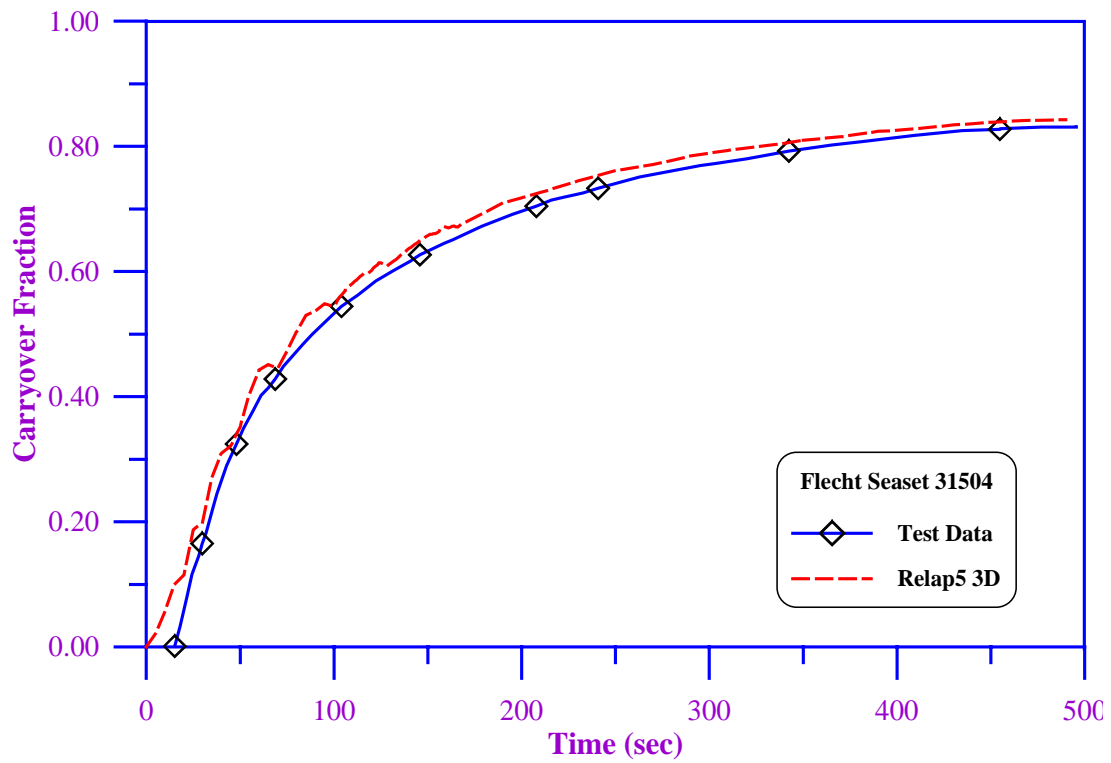


Figure 9. Comparison of Measured and Calculated Carryover Fractions

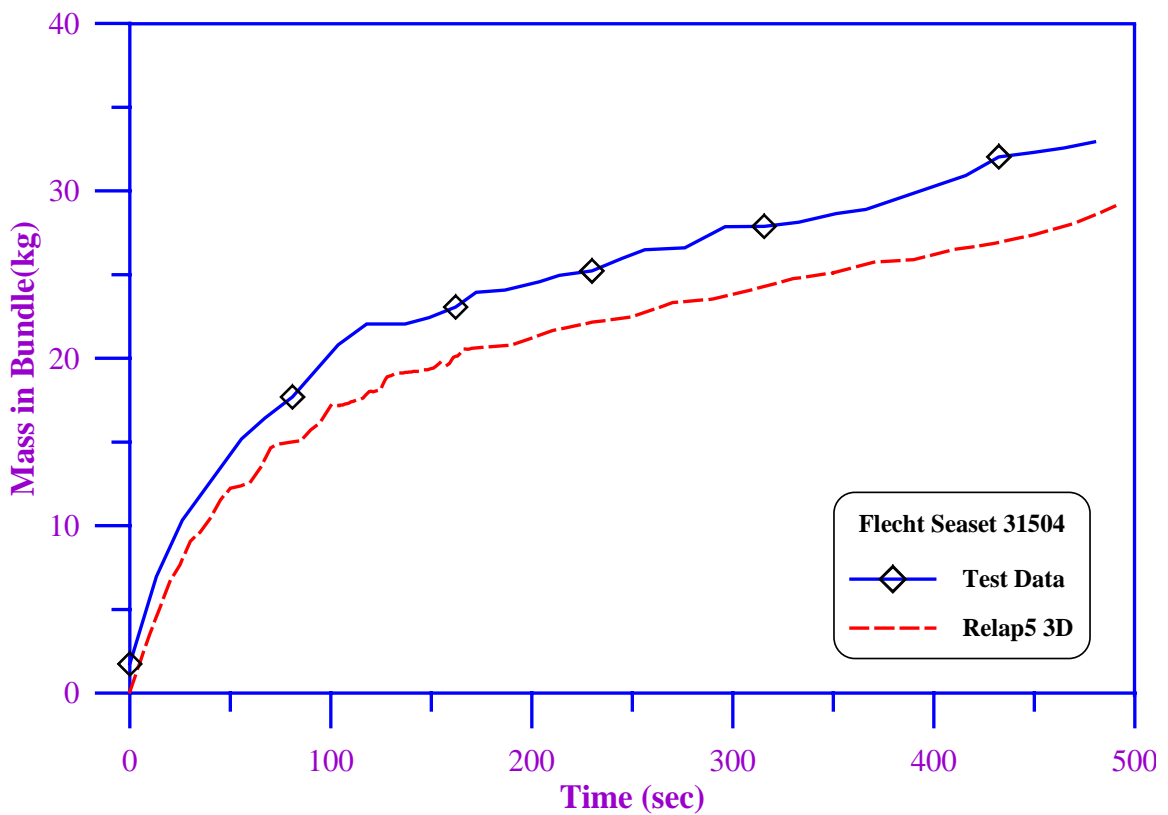


Figure 10. Comparison of Measured and Calculated Bundle Masses

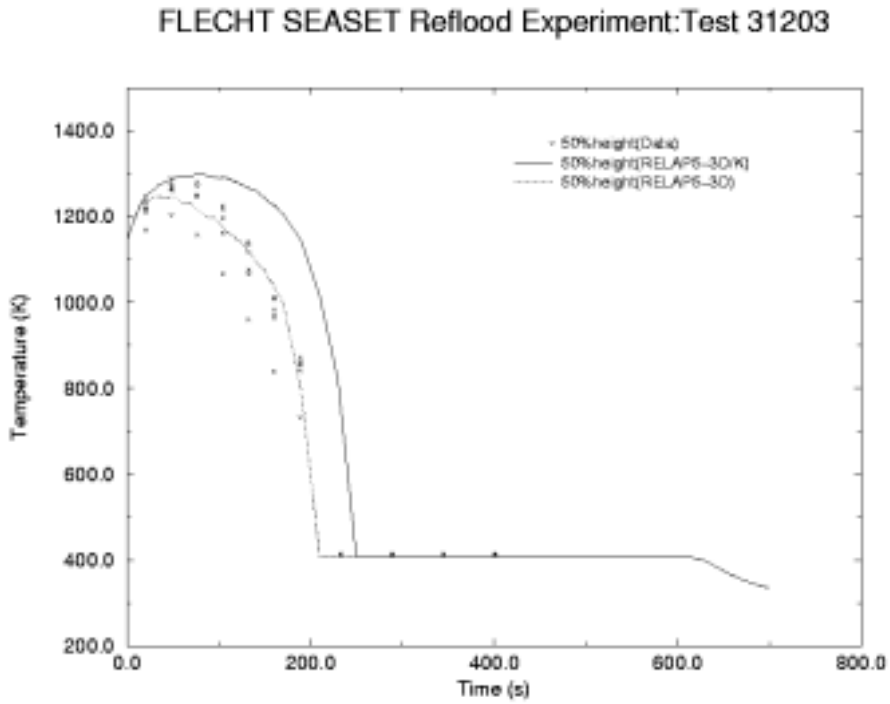


Figure 11. Comparison of Measured and Calculated Peak Cladding Temperatures

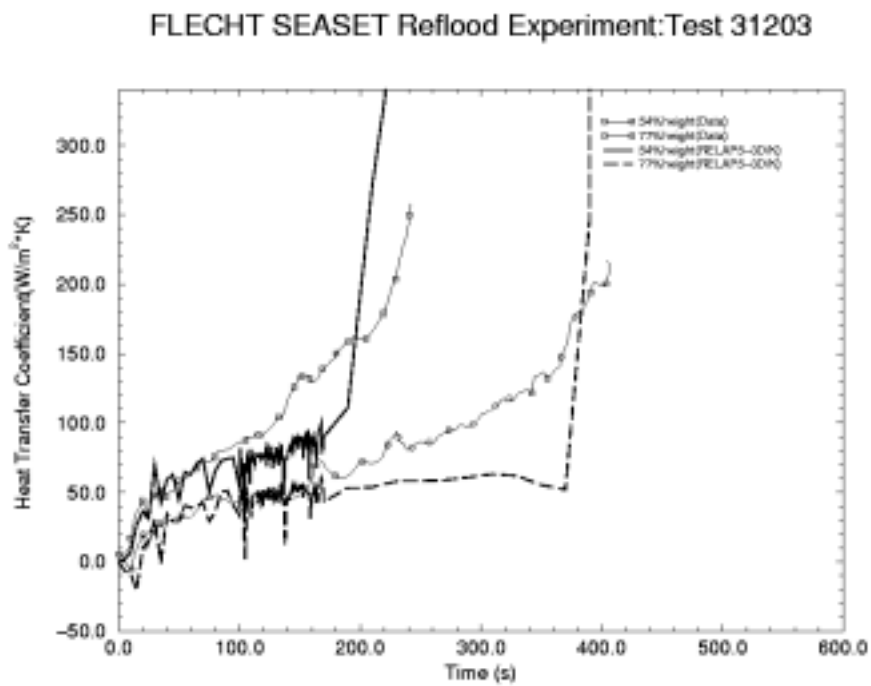


Figure 12. Comparisons of Measured and Calculated Heat Transfer Coefficients

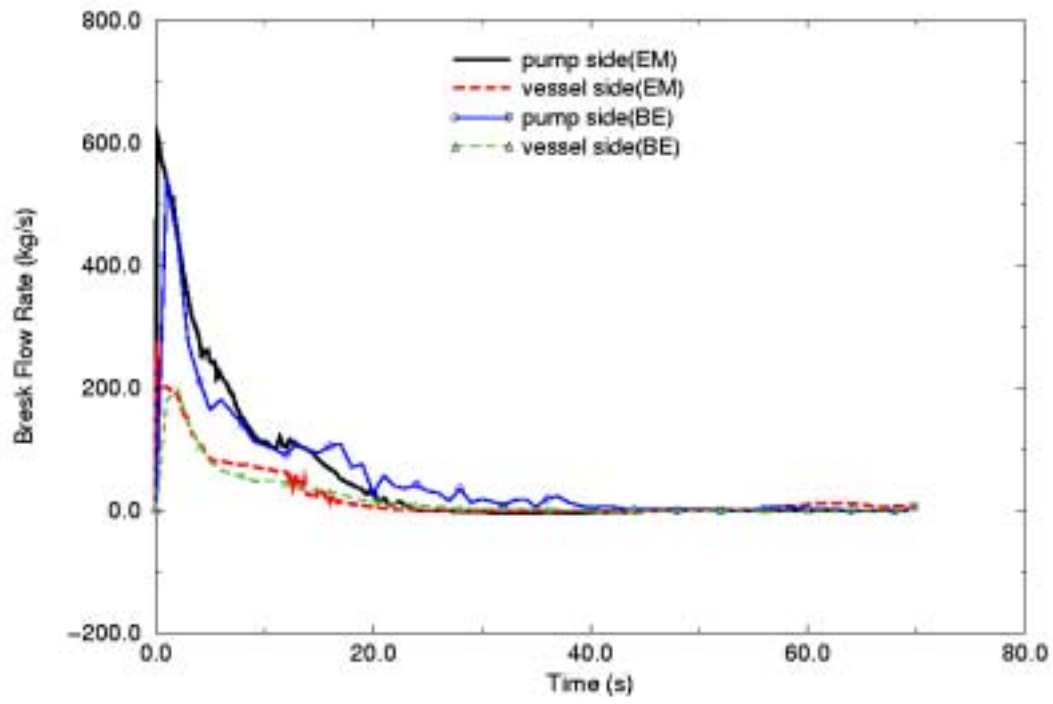


Figure 14. Comparison of System Pressures of L2-5

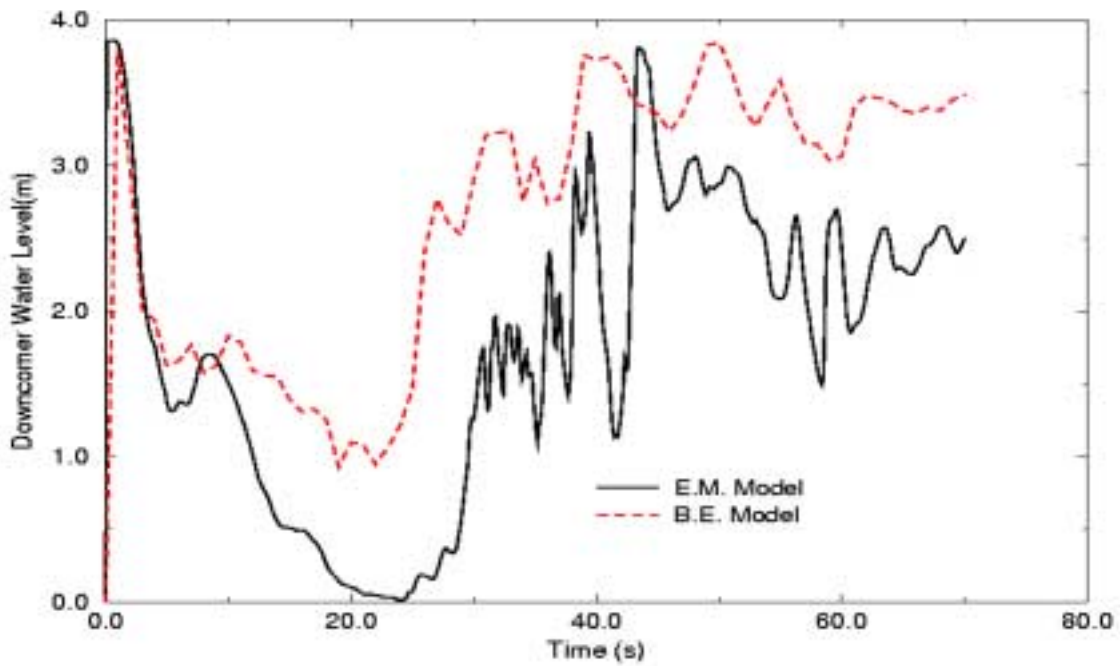
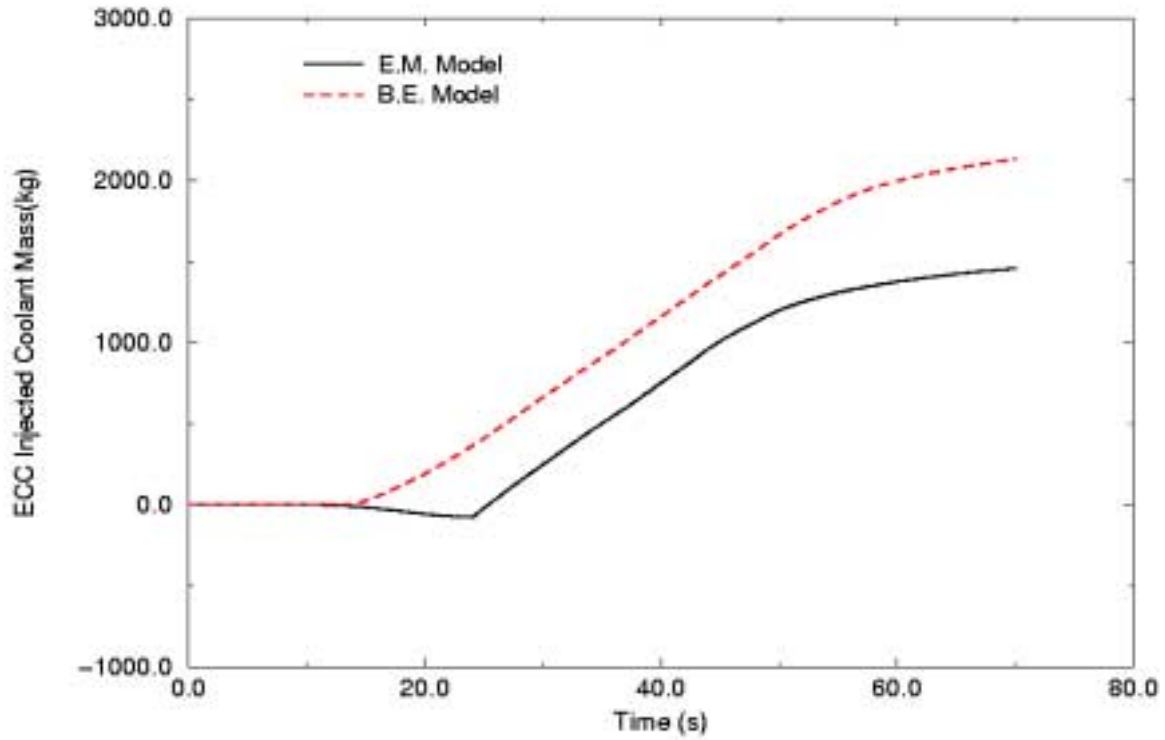


Figure 16. Comparison of Water Levels in Downcomer of L2-5

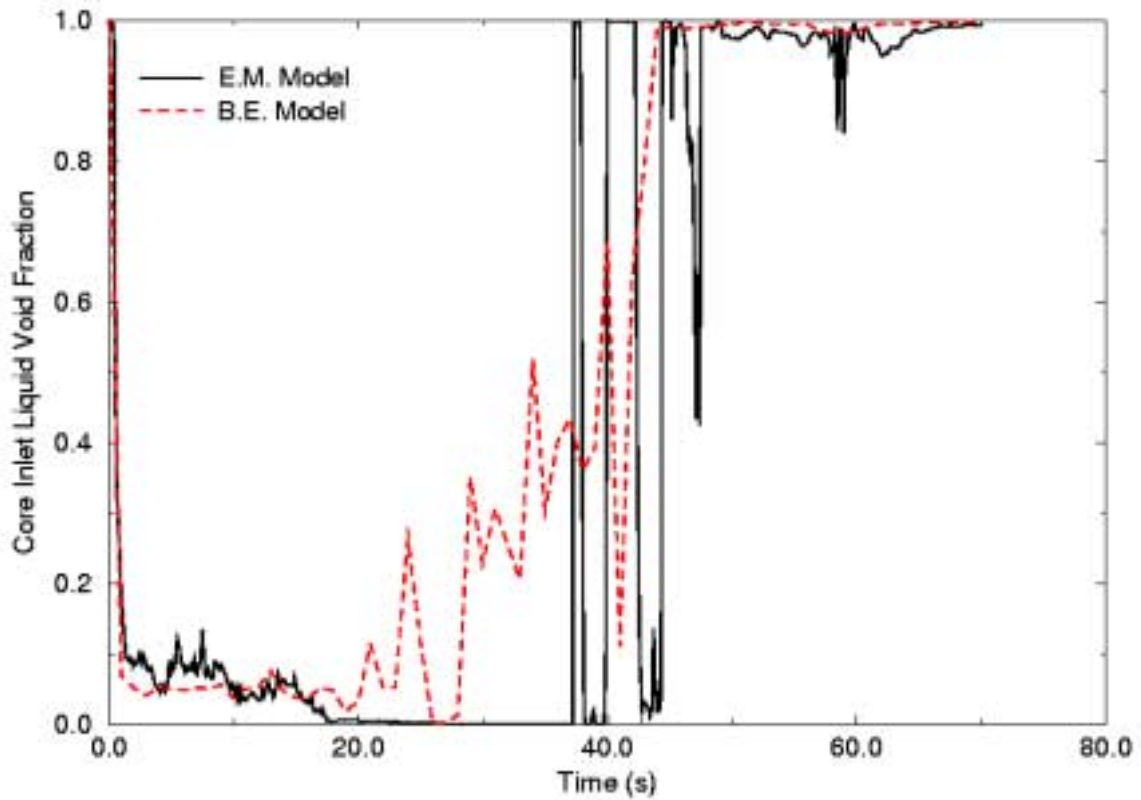


Figure 17. Comparison of Core Inlet Liquid Void Fraction of L2-5

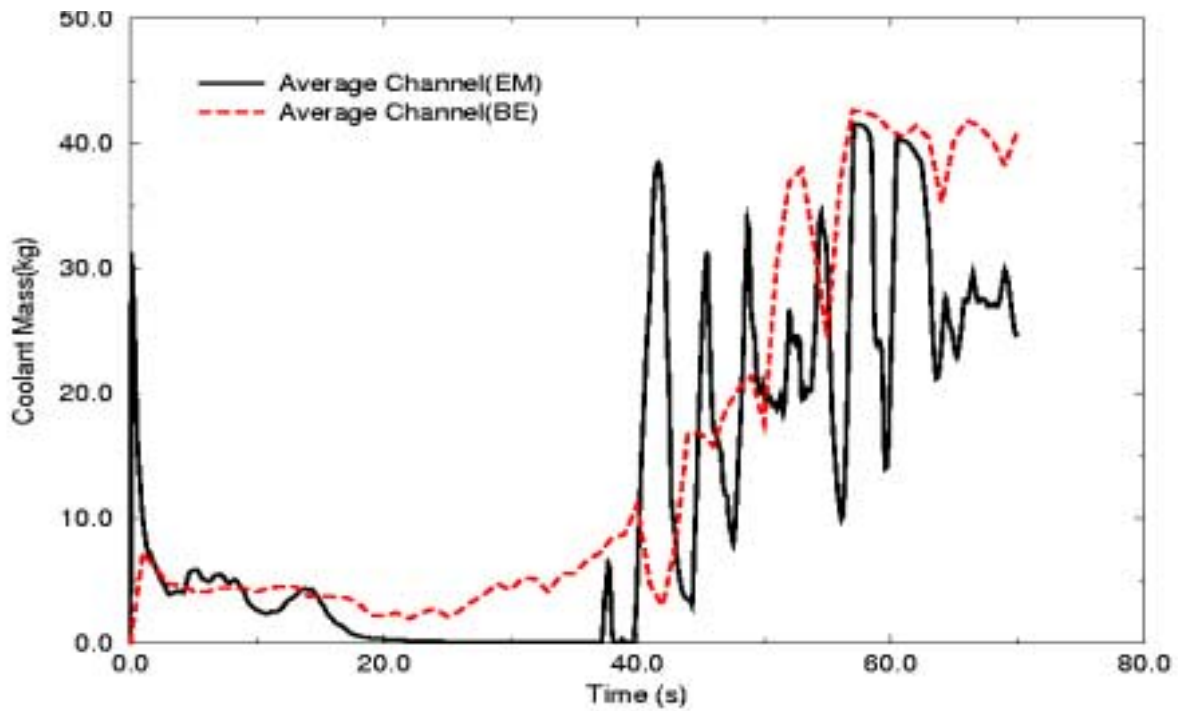


Figure 18. Comparison of Reactor Average Channel Coolant Mass of L2-5

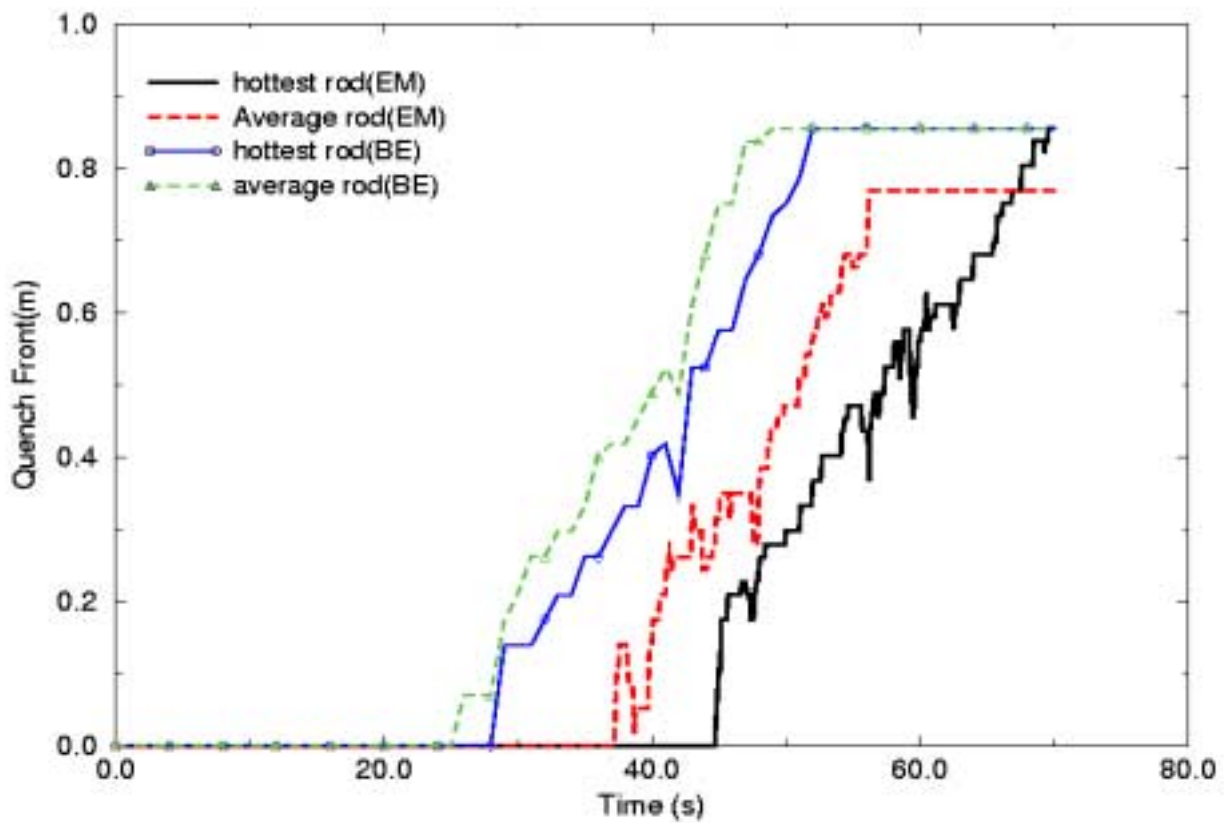


Figure 19. Comparison of Quench Front Movements of L2-5

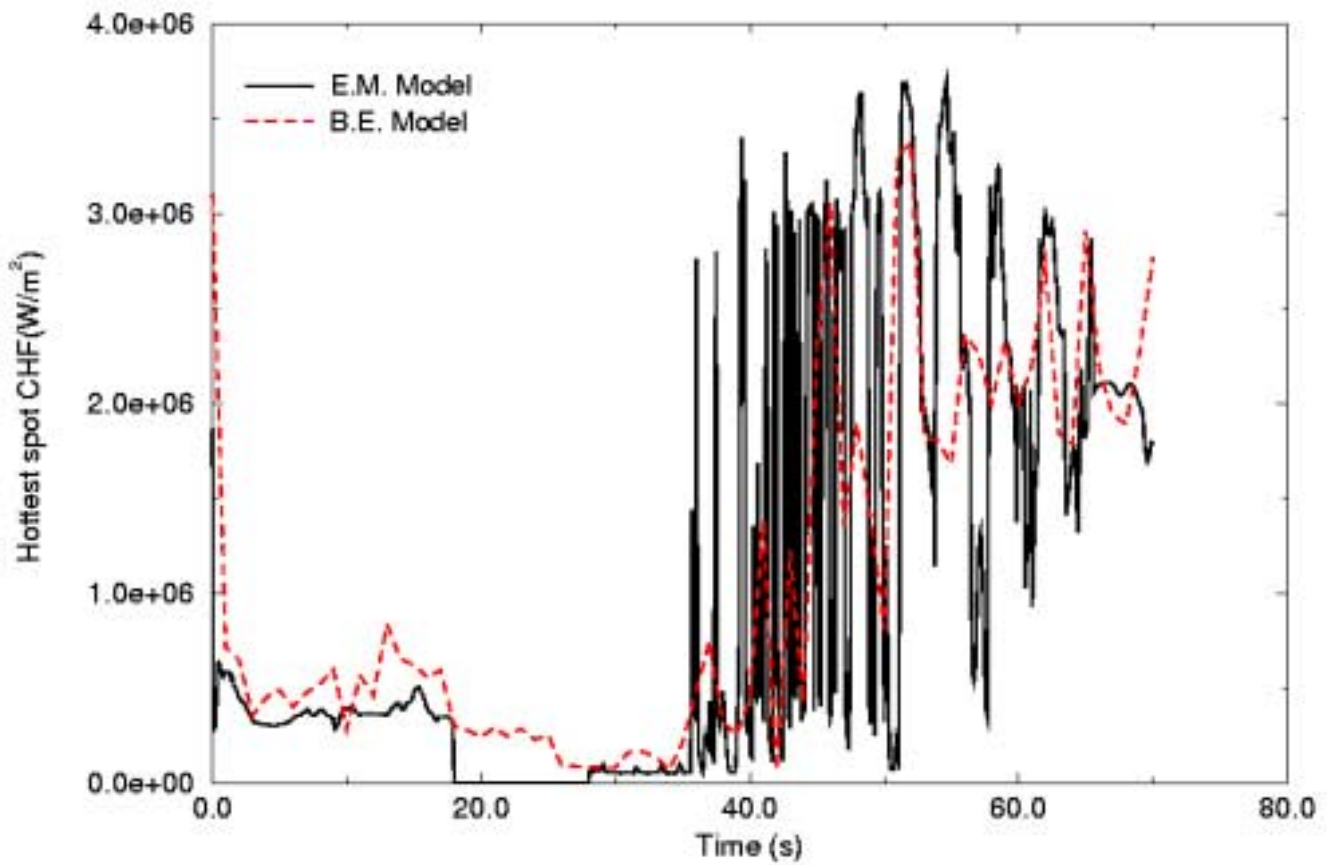


Figure 20. Comparison of CHF on the Hot Spot of L2-5

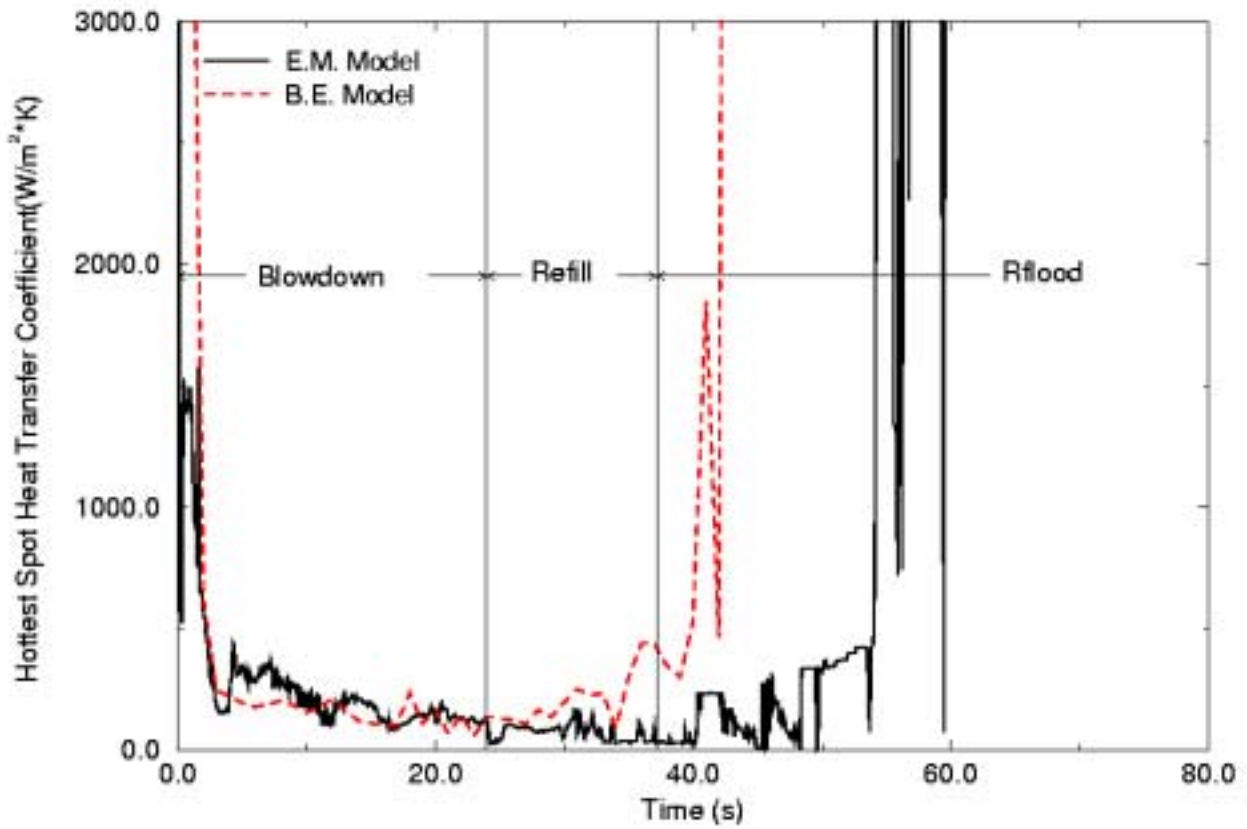


Figure 21. Heat Transfer Coefficients on the Hot Spot of L2-5

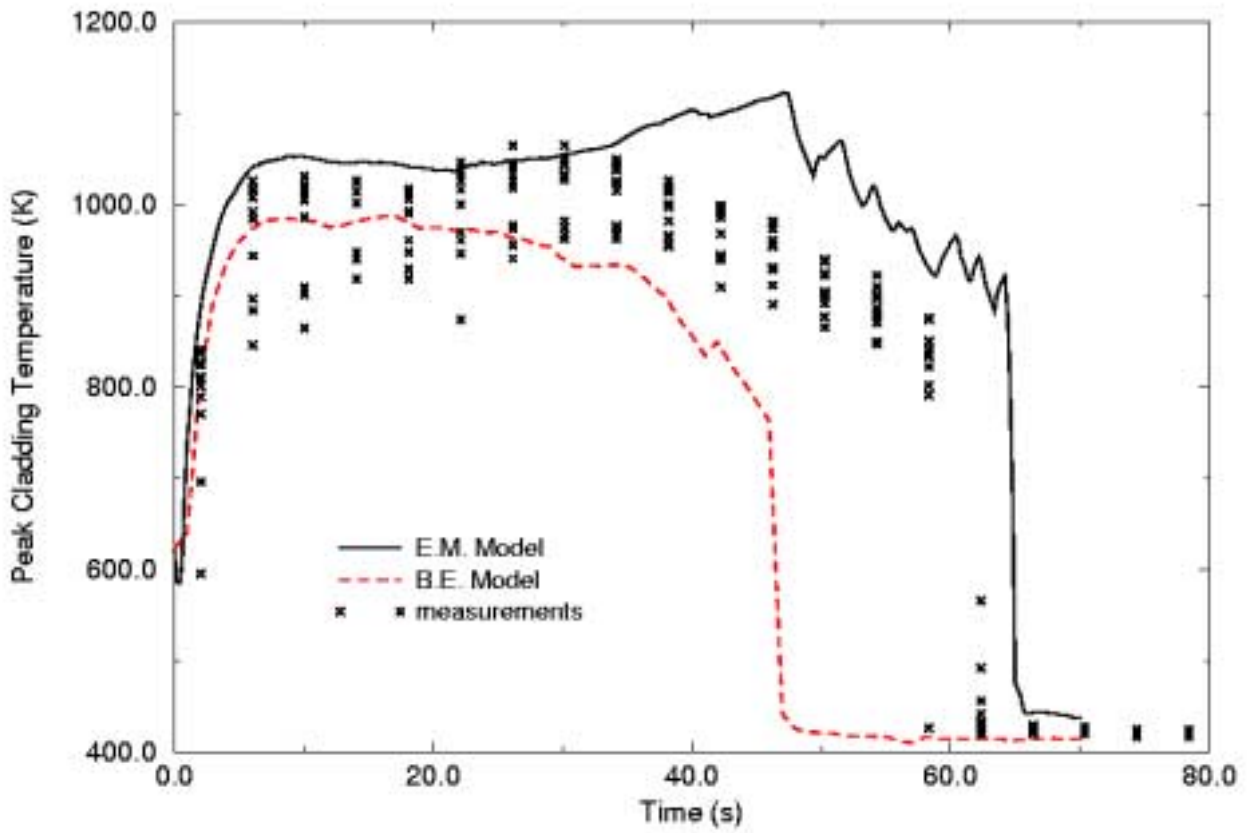


Figure 22. Comparison of PCT on the Hot Spot of L2-5

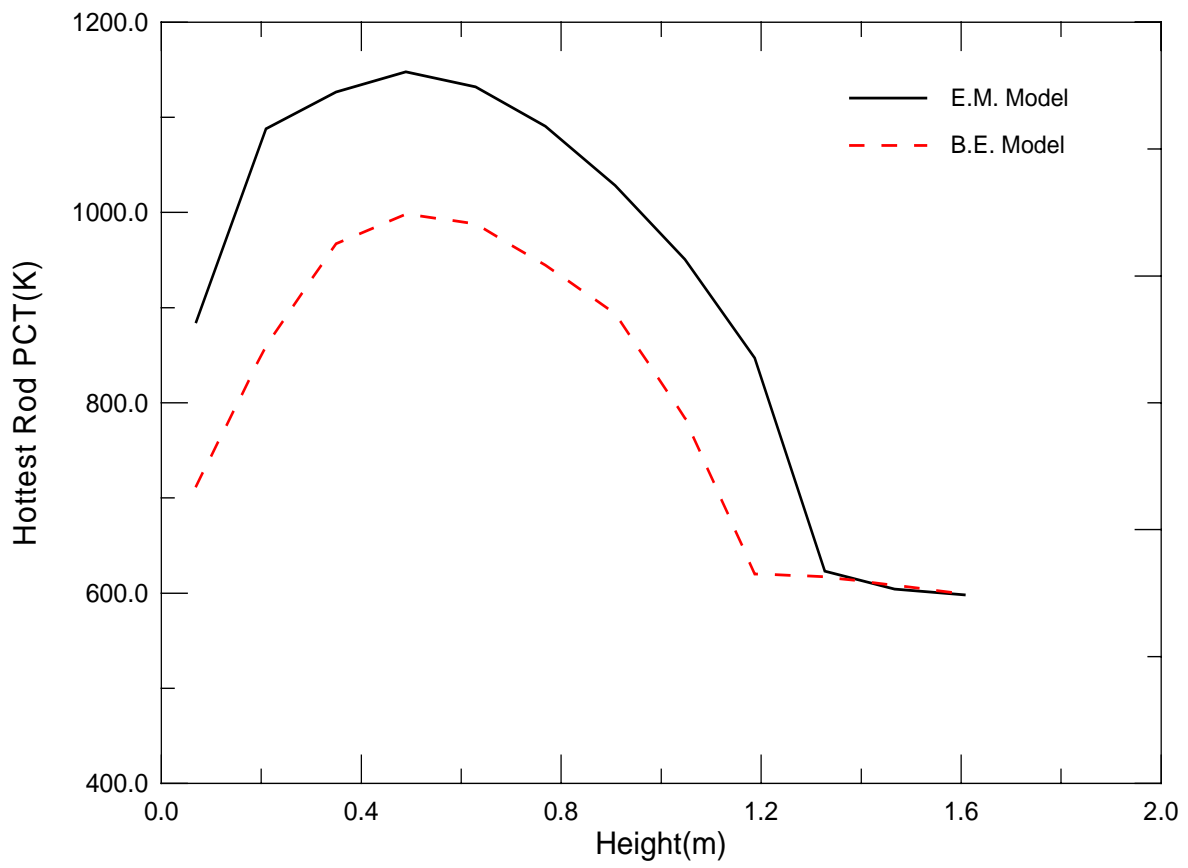


Figure 23. Comparison of PCT along the Hot Rod Elevation of L2-5

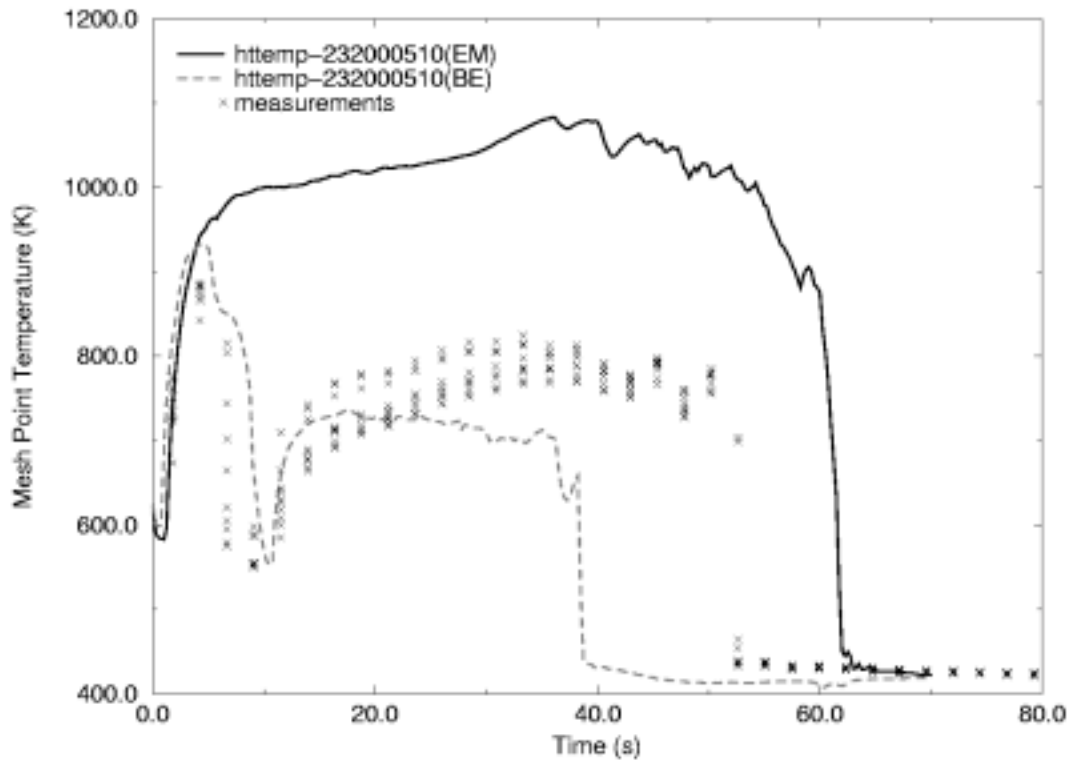


Figure 24. Comparison of PCT on the Hot Spot of L2-3

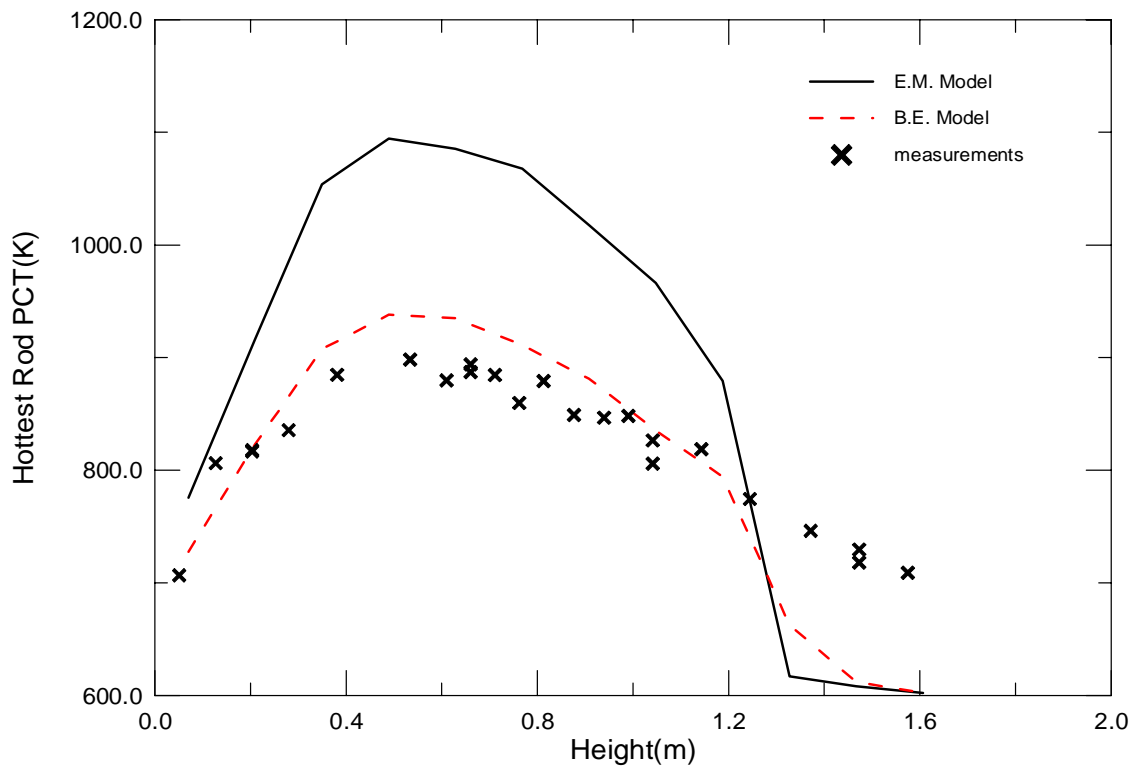


Figure 25. Comparison of PCT along the Hot Rod Elevation of L2-3

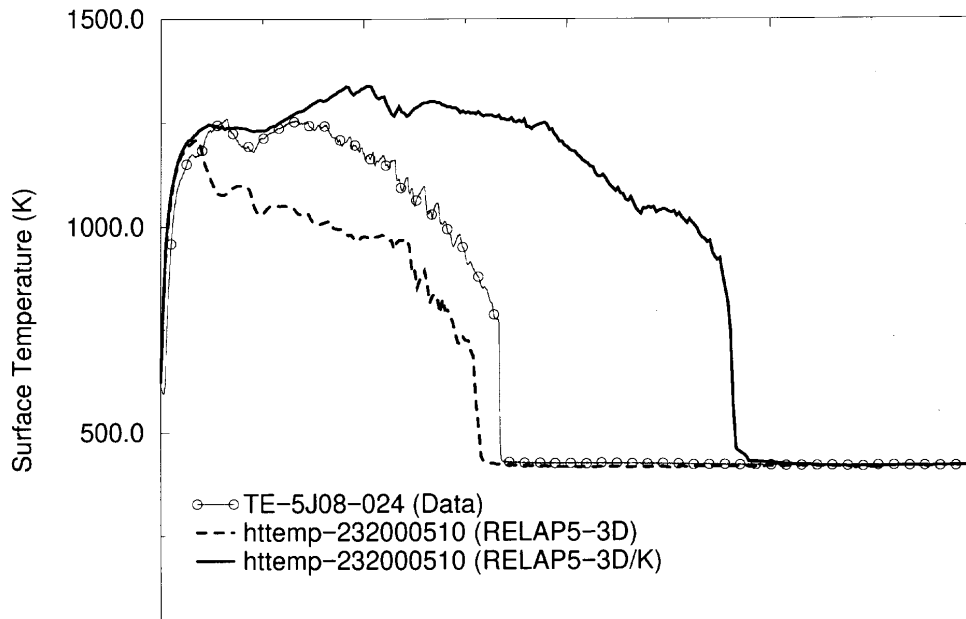


Figure 26. Comparison of PCT on the Hot Spot of LP-LB-1

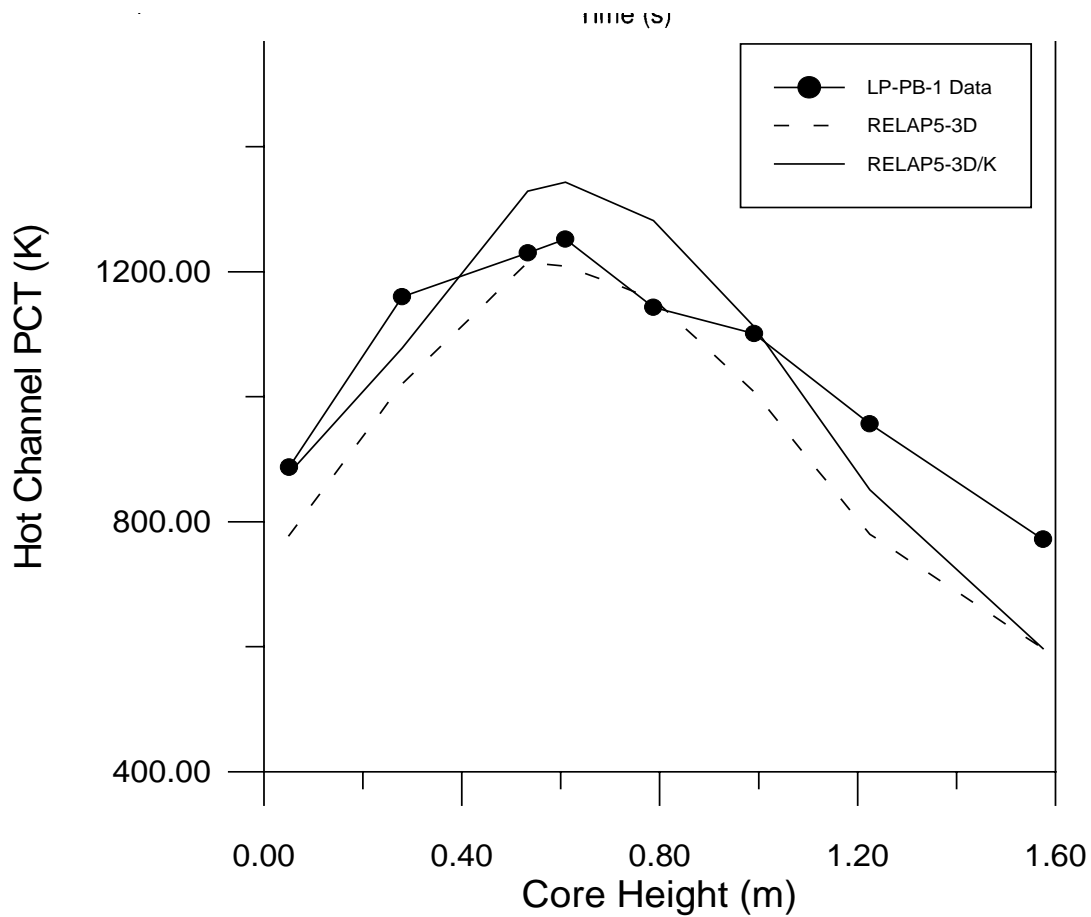


Figure 27. Comparison of PCT along the Hot Rod Elevation

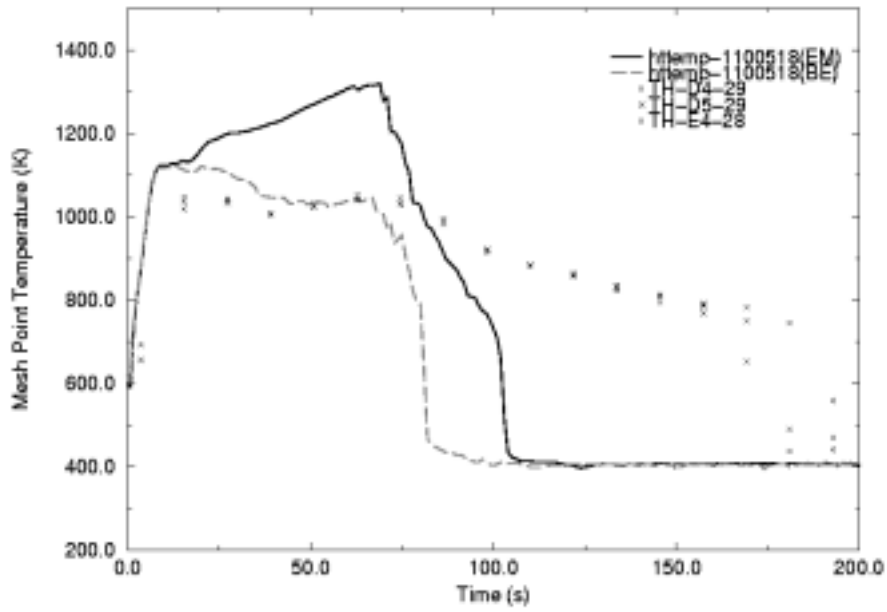


Figure 28. Comparison of PCT on the Hot Spot of S-06-3

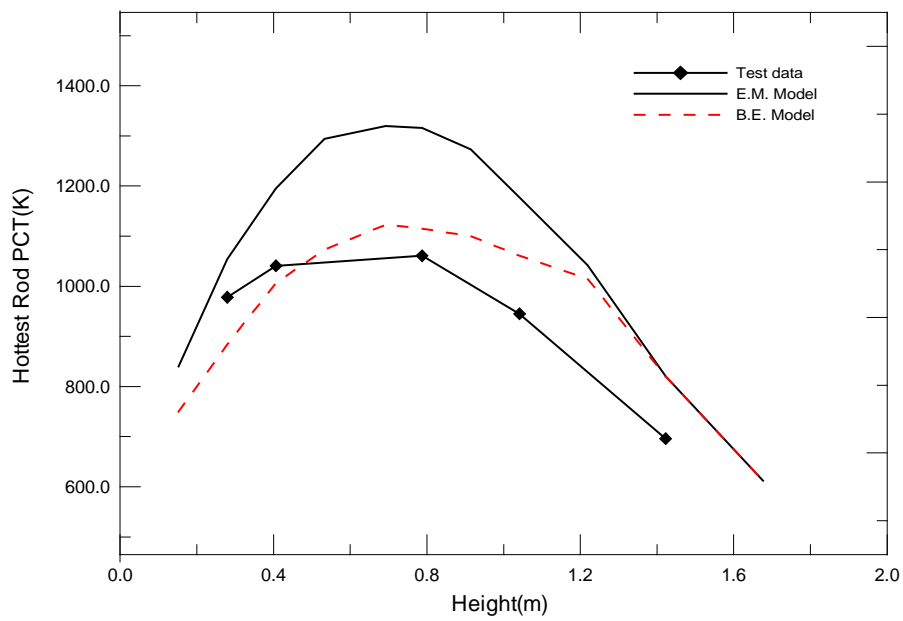


Figure 29. Comparison of PCT along the Hot Rod Elevation

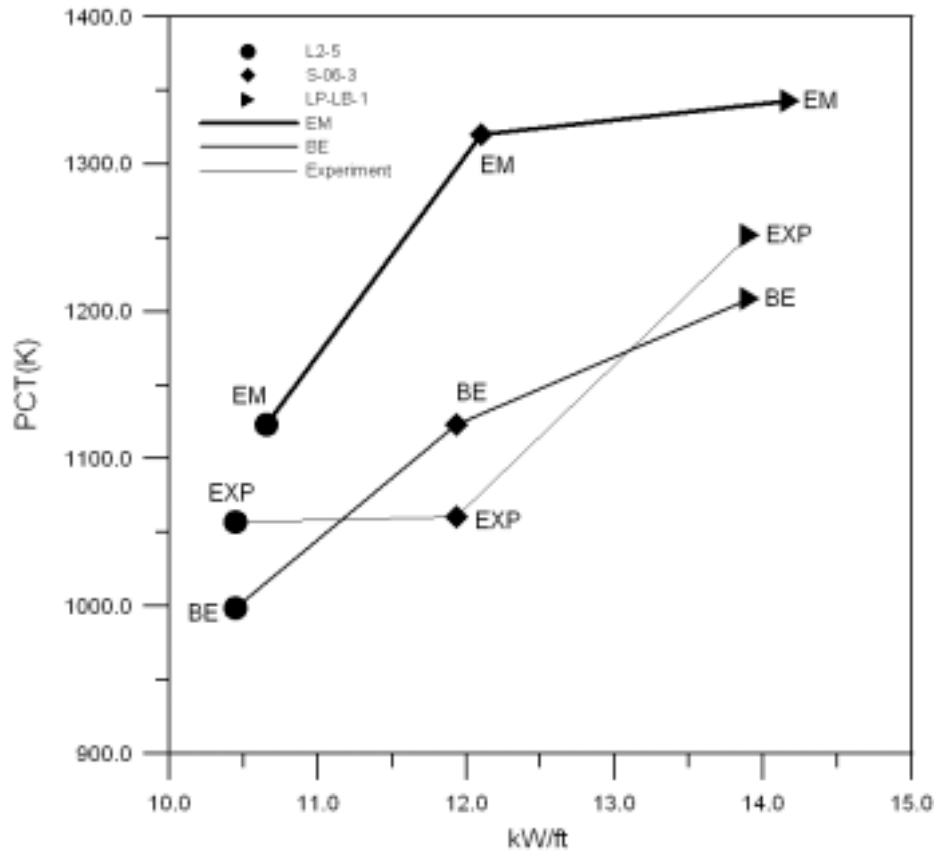


Figure 30. Comparison of Resulted PCTs from EM, BE and Experiments

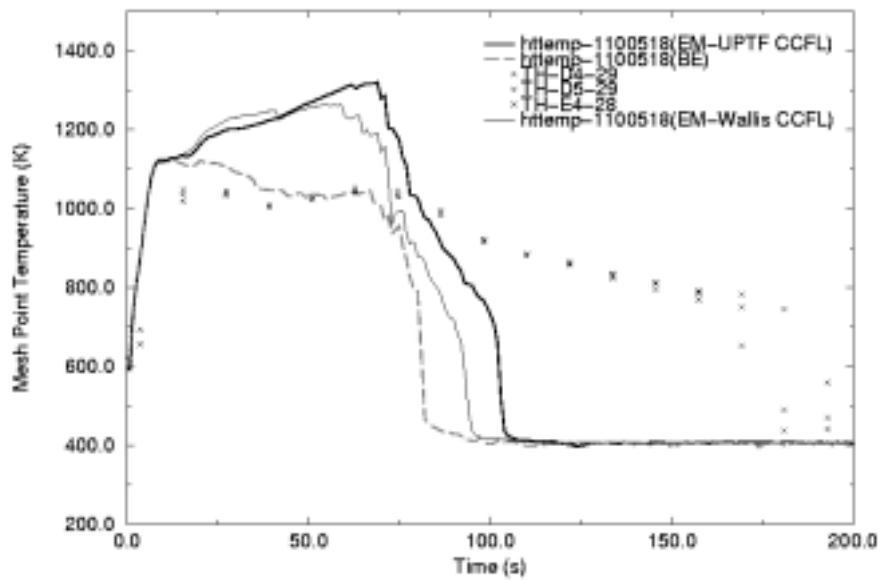


Figure 31. Effect of CCFL on PCT Calculation for S-06-3